Design and Evaluation of Compact Multi-antennas for Efficient MIMO Communications

Tian, Ruiyuan

2011

Design and Evaluation of Compact Multi-antennas for Efficient MIMO Communications

Doctoral Dissertation

Ruiyuan Tian

Lund University
Lund, Sweden
2011

Academic thesis which, by due permission of the Faculty of Engineering at Lund University, will be publicly defended on Tuesday, November 29, 2011, at 10.15 in lecture hall E:1406 of the E Building, Dept. of Electrical and Information Technology, Ole Römers väg 3, Lund, for the degree of Doctor of Philosophy in Engineering.

Department of Electrical and Information Technology
Lund University
P.O. Box 118, SE-221 00 Lund, Sweden

This thesis is set in Computer Modern 10pt
with the LaTeX Documentation System

Series of licentiate and doctoral theses
ISSN 1654-790X; No. 35
ISBN 978-91-7473-186-6

Printed in Sweden by *Tryckeriet i E-huset*, Lund.
October 2011.

. . . to Yuanyuan and our parents . . .

Abstract

The use of multi-antenna systems with multiple-input multiple-output (MIMO) technology will play a key role in providing high spectrum efficiency for next generation mobile communication systems. This thesis offers valuable insights on the design of compact multi-antennas for efficient MIMO communications. In the course of the thesis work, several novel six-port antenna designs have been proposed to simultaneously exploit all six possible degrees-of-freedom (DOFs) by means of various antenna diversity mechanisms (Paper I & II). Moreover, the thesis also examines the potential of using uncoupled matching networks to adaptively optimize compact multi-antenna systems to their dynamic usage environments (Paper III). Furthermore, a simple and intuitive metric is proposed for evaluating the performance of MIMO antennas when operating in the spatial multiplexing mode (Paper IV). Last but not least, cooperation among multi-antenna systems at all three sectors of a given cellular base station is shown to deliver significant benefit at sector edges (Paper V). The thesis with the five included research papers extend the understanding of MIMO systems from an antenna and propagation perspective. It provides important guidelines in designing compact and efficient MIMO antennas in their usage environments.

In Paper I, a fundamental question on the number of effective DOFs in a wireless channel is explored using two co-located six-port antenna arrays. The antenna elements of both arrays closely reproduce the desired characteristics of fundamental electric and magnetic dipoles, which can efficiently extract angle and polarization diversities from wireless channels. In particular, one of the two array designs is by far the most electrically compact six-port antenna structure in the literature. Analysis of measured channel eigenvalues in a rich multi-path scattering environment shows that six eigenchannels are successfully attained for the purpose of spatial multiplexing.

To study the potential of implementing different diversity mechanisms on a practical multi-port antenna, Paper II builds on an existing dielectric resonator antenna (DRA) to provide a compact six-port DRA array that jointly utilizes

space, polarization and angle diversities. In order to fully substantiate the practicality of the DRA array for indoor MIMO applications, the compact DRA array together with two reference but much larger arrays were evaluated in an office scenario. The use of the compact DRA array at the receiver is shown to achieve comparable performance to that of the reference monopole array due to the DRA array's rich diversity characteristics.

In Paper III, the study of uncoupled matching networks to counteract mutual coupling effects in multi-antenna systems is extended by allowing for unbalanced matching impedances. Numerical studies suggest that unbalanced matching is especially effective for array topologies whose effective apertures can vary significantly with respect to the propagation channel. Moreover, it is also demonstrated that unbalanced matching is capable of adapting the radiation patterns of the array elements to the dynamic propagation environment.

Paper IV introduces multiplexing efficiency as a performance metric which defines the loss of efficiency in decibel when using a multi-antenna prototype under test to achieve the same multiplexing performance as that of an ideal array in the same propagation environment. Its unique features are both its simplicity and the valuable insights it offers with respect to the performance impacts of different antenna impairments in multi-antenna systems.

In Paper V, intrasite cooperation among three 120°-sector, each with a cross-polarized antenna pair, is investigated in a measured urban macrocellular environment. The single-user capacity improvement is found to exceed 40% at the sector edges, where improvements are most needed. In addition, a simple simulation model is developed to analyze the respective impact of antennas and specific propagation mechanisms on the measured cooperative gain.

Preface

After completing the course work component of my Master of Science degree program, which concerns digital communication systems and technologies, a thesis work on radio channel modeling brought me into the world of MIMO. To my understanding, MIMO has been one of the hottest research topics in radio communications over the past decade. When I finished my master's thesis project, I felt that I had learned something about MIMO and wondered if there were still exciting opportunities left in this research field. As it turned out, despite extensive research in MIMO technology, surprisingly little effort has been directed towards assessing and mitigating the impacts of different antenna impairments on the performance of MIMO systems in their realistic usage conditions. In this context, the overarching question that this thesis tries to answer is: how should we design and evaluate compact multi-antennas that can deliver efficient MIMO communications?

The thesis is a compilation of an introduction to the research field and a summary of my contributions, together with five research papers that present the main results achieved during my graduate study. It extends the understanding of MIMO systems from an antenna and propagation perspective, and offers valuable insights on the design of compact yet efficient multi-antennas. The included papers are:

[1] R. Tian and B. K. Lau, "Experimental verification of degrees of freedom for co-located antennas in wireless channels," submitted to *IEEE Transactions on Antennas and Propagation*, Jun. 2011 (revised Oct. 2011).

[2] R. Tian, V. Plicanic, B. K. Lau, and Z. Ying, "A compact six-port dielectric resonator antenna array: MIMO channel measurements and performance analysis," *IEEE Transactions on Antennas and Propagation*, vol. 58, no. 4, pp. 1369 – 1379, Apr. 2010.

[3] R. Tian and B. K. Lau, "Uncoupled antenna matching for performance optimization in compact MIMO systems using unbalanced load impedance,"

in *Proc. IEEE Vehicular Technology Conference (VTC Spring 2008)*, pp. 299 – 303, Singapore, May 11 – 14, 2008.

[4] R. Tian, B. K. Lau, and Z. Ying, "Multiplexing efficiency of MIMO antennas," *IEEE Antennas and Wireless Propagation Letters*, vol. 10, pp. 183 – 186, 2011.

[5] R. Tian, B. Wu, B. K. Lau, and J. Medbo, "On MIMO performance enhancement with multi-sector cooperation in a measured urban environment," submitted to *Electronics Letters*, 2011.

During my graduate study, I have also contributed to the following publications, that are not included in the thesis:

[6] R. Tian, B. K. Lau, and Z. Ying, "Multiplexing efficiency of MIMO antennas in arbitrary propagation scenarios," submitted to *6th European Conference on Antennas and Propagation (EuCAP)*, Mar. 2012.

[7] R. Tian, B. K. Lau, and J. Medbo, "Impact of Rician fading and cross-polarization ratio on the orthogonality of dual-polarized wireless channels," submitted to *6th European Conference on Antennas and Propagation (EuCAP)*, Mar. 2012.

[8] V. Plicanic, I. Vasilev, R. Tian, and B. K. Lau, "On capacity maximisation of a handheld MIMO terminal with adaptive matching in an indoor environment," *Electronics Letters*, vol. 47, no. 16, pp. 900 – 901, 2011.

[9] R. Tian and B. K. Lau, "Degree-of-freedom evaluation of six-port antenna arrays in a rich scattering environment," in *Proc. IEEE International Symposium on Antennas and Propagation*, vol. 1, pp. 51 – 54, Spokane, USA, Jul. 2011.

[10] R. Tian and B. K. Lau, "Simple and improved approach of estimating MIMO capacity from antenna magnitude patterns," in *Proc. 3rd European Conference on Antennas and Propagation (EuCAP)*, Berlin, Germany, Mar. 2009.

[11] R. Tian, V. Plicanic, B. K. Lau, J. Långbacka, and Z. Ying, "MIMO performance of diversity-rich compact six-port dielectric resonator antenna arrays in measured indoor environments at 2.65 GHz," in *Proc. 2nd COST2100 Workshop - Multiple Antenna Systems on Small Terminals (Small and Smart)*, Valencia, Spain, May 2009.

[12] B. K. Lau and R. Tian, "Antenna matching for performance optimization in compact MIMO systems," in *Proc. Microwave Workshops and Exhibition (MWE)*, Japan, Nov. 2007.

The research results throughout my graduate study have also been presented as temporary documents (TDs) in the European Cooperation in Science and Technology (COST) Action 2100 and IC1004:

[13] R. Tian, B. K. Lau, and Z. Ying, "Multiplexing efficiency of multiple antenna systems," in *COST IC1004*, TD(11)01025, Lund, Sweden, Jun. 2011.

[14] R. Tian and B. K. Lau, "Six-port antennas for experimental verification of six degrees-of-freedom in wireless channels," in *COST2100*, TD(10)12054, Bologna, Italy, Nov. 2010.

[15] R. Tian and B. K. Lau, "Correlation-based phase synthesis approach for MIMO capacity prediction using antenna magnitude patterns," in *COST2100*, TD(09)727, Braunschweig, Germany, Feb. 2009.

[16] R. Tian and B. K. Lau, "On prediction of MIMO capacity performance with antenna magnitude patterns," in *COST2100*, TD(08)651, Lille, France, Oct. 2008.

[17] R. Tian and B. K. Lau, "On compact MIMO antenna systems with optimized uncoupled impedance matching," in *COST2100*, TD(08)438, Wroclaw, Poland, Feb. 2008.

As a result of my active involvement in COST2100, I have been a contributor to the COST2100 final report, which will be published as:

[18] R. Verdone and A. Zanella, *Pervasive Mobile & Ambient Wireless Communications - The COST Action 2100*, Springer. (In press)

Acknowledgments

Looking back at my life as a graduate student, I am grateful to many people. Without their generous support, this thesis would not have been possible. I owe my gratitude to all of them.

First and foremost, I would like to express my deepest gratitude to Assoc. Prof. Buon Kiong Lau for giving me the opportunity to pursuit a Ph.D. under his guidance. I am grateful for his insightful discussions, constant encouragement, helpful professional advice, and critical suggestions on my manuscripts. His extensive knowledge and high ambitions have been an important source of inspiration for me to overcome challenges along the way. As an ancient Chinese saying puts it, *"Once you have been my teacher for a day, you are my teacher for a lifetime"*.

Secondly, I am grateful to a number of my colleagues. In particular, I sincerely thank my officemates, Dr. Vanja Plicanic Samuelsson and Ivaylo Vasilev. Our close collaborations have truly been pleasant and memorable experiences, even during several tedious yet exciting measurement campaigns. I am also grateful to Prof. Andreas F. Molisch for being my co-supervisor in the starting phase of my research, Assoc. Prof. Fredrik Tufvesson and Dr. Shurjeel Wyne for advising me in channel measurements, Prof. Gerhard Kristensson for teaching me electromagnetic theory, and Assoc. Prof. Anders J. Johansson, Prof. Mats Gustafsson and Dr. Richard Lundin for guiding me as their teaching assistant. Moreover, I am also indebted to Göran Jönsson for training my RF measurement skills, Martin Nilsson and Lars Hedenstjerna for their kind and critical engineering support on numerous occasions. Further, I would like to acknowledge Dr. Anders Derneryd, Fredrik Harrysson, Prof. Jørgen B. Andersen and Prof. Michael A. Jensen for providing fruitful suggestions during their short but frequent visits to Lund. Thanks are also due to my past and present fellow Ph.D. students for their support in all aspects, in particular Marius Cismasu, Dr. Andrés A. Glazunov and Dr. Christian Sohl for sharing their knowledge, Dr. Alireza Kazemzadeh and Rohit Chandra for our cooperation in teaching, and Anders Bernland for his help in improving my Swedish sum-

mary of this thesis. I also thank Hui Li for the interesting discussions during her visits here, and several students that I have cooperated with, especially Jonas Långbacka, Yi Tan and Bo Wu. Furthermore, I sincerely thank Pia Bruhn, Doris Glöck, Elisabeth Nordström, Birgitta Holmgren and Elsbieta Szybicka for taking care of administrative issues, and Josef Wajnblom, Bertil Lindvall, Erik Jonsson and Richard Blohm for providing IT support. I am also grateful to Prof. Anders Karlsson for his help, and Dr. Bo Peterson for being my mentor.

Thanks to Thomas Bolin and Dr. Peter C. Karlsson, I have been very fortunate to receive generous assistance from Sony Ericsson Mobile Communications AB in Lund during my thesis work. My gratitude goes to Dr. Vanja Plicanic Samuelsson for making necessary arrangements for performing different measurement tasks, Dr. Dmytro Pugachov for his help with antenna measurements, and Zhinong Ying for our co-authored papers. I also thank Dr. Jonas Medbo of Ericsson Research for contributing to our joint publications.

I would also like to thank Prof. Daniel D. Stancil for taking the time to be the faculty opponent of my thesis, Prof. Gert F. Pedersen, Dr. Mattias Frenne and Assoc. Prof. Marco D. Migliore for agreeing to be the grading committee members.

Last but not least, I would like to express my gratitude to all my Chinese friends in Lund and Sweden, who make me feel like home. I am especially grateful to Dr. Zhuo Zou and Dr. Haiying Cao for sharing the experiences of Ph.D. student life, Jing Wang for discussing the state of the art while playing basketball, and Meifang Zhu, Tao Tao, Yusheng Liu and Lu Zhang for appreciating my cooking. Very importantly, I sincerely thank my parents for their love. Another ancient Chinese saying has it that *"While your parents are alive, do not journey afar. If a journey has to be made, your direction must be told"*. This thesis is dedicated to them, as my answer to the direction taken. Finally, for her true love, strong faith in me, endless patience and understanding, I give these special words to the love of my life, Yuanyuan: Regardless of the direction this journey of life is taking us, we will always be together.

This work has been financially supported by VINNOVA (Grant no. 2007-01377, 2008-00970 and 2009-04047). Travel grants from Kungliga Fysiografiska Sällskapet in Lund and Ericsson Research Foundation are also acknowledged.

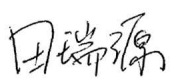

Ruiyuan Tian

October 2011

List of Acronyms and Abbreviations

2D Two Dimensional

3D Three Dimensional

AOA Angle-Of-Arrival

AOD Angle-Of-Departure

AP Access Point

APS Angular Power Spectrum

AWGN Additive White Gaussian Noise

BC Broadcast Channel

BPR Branch Power Ratio

BS Base Station

CCDF Complementary Cumulative Distribution Function

CDF Cumulative Distribution Function

CoMP Coordinated Multi-Point

CPR Co-Polarization Ratio

CSI Channel State Information

DAS Distributed Antenna System

DOF Degree-Of-Freedom

DPC Dirty Paper Coding

DRA Dielectric Resonator Antenna

EDOF Effective Degree-Of-Freedom

IID Independent and Identically Distributed

LD Laser Diode

LOS Line-Of-Sight

LTE Long Term Evolution

MAC Multiple Access Channel

MEG Mean Effective Gain

MIMO Multiple-Input Multiple-Output

MPC Multi-Path Component

MS Mobile Station

NLOS Non-Line-Of-Sight

OTA Over-The-Air

PCB Printed Circuit Board

PD Photo Diode

PIFA Planar Inverted F Antenna

RC Reverberation Chamber

RF Radio Frequency

ROF Radio Over Fiber

RX Receive

SDMA Space Division Multiple Access

SISO Single-Input Single-Output

SM Spatial Multiplexing

SNR Signal to Noise Ratio

SRR Split Ring Resonator

TE Transverse Electric

TIS Total Isotropic Sensitivity

TM Transverse Magnetic

TRP Total Radiated Power

TX Transmit

ULA Uniform Linear Array

UTA Uniform Triangular Array

VNA Vector Network Analyzer

WLAN Wireless Local Area Network

XPD Cross-Polarization Discrimination

XPR Cross-Polarization Ratio

Contents

Part I

Overview of the Research Field

Chapter 1

Introduction

The evolution of technology for transmitting and receiving information by means of electromagnetic wave propagation has gone a long way. The author of this thesis does not intend to describe every advancement along the road map since Guglielmo Marconi's pioneering experiment. Instead, the scope of this introduction is mainly focused on a core technology, multiple-input multiple-output (MIMO) wireless communication, which is an integral part of both new and upcoming mobile communication systems.

The desire of higher data transmission rates has been the driving force behind major advancements in wireless technology. However, the maximum possible data rate of a communication system is fundamentally limited by the Shannon capacity of the communication channel [1]. In order to achieve not only higher peak data rates but also higher rates over entire coverage area, the research and development of next generation mobile systems known as the International Mobile Telecommunication (IMT)-Advanced systems is underway worldwide [2]. Multi-antenna systems with MIMO technology will play a key role in providing the target data rate of 1 Gbps with high spectrum efficiency. From arguably the very first known multi-antenna system, in the form of Guglielmo Marconi employing a physically massive four-element circular antenna array for his transatlantic radio transmissions in 1901 [3], MIMO technology has come a long way. This introduction will briefly discuss why MIMO has become known as "a key to gigabit wireless" [4] and the key issues to be addressed from an antenna and propagation perspective to enable efficient MIMO communications.

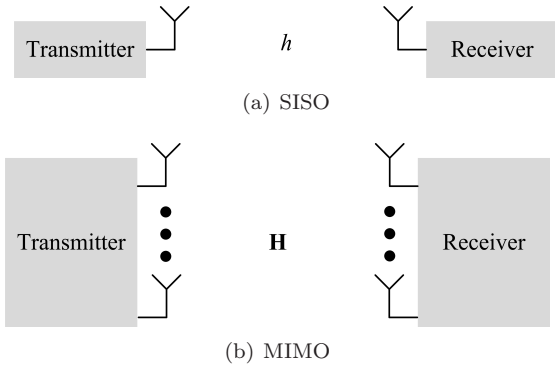

(a) SISO

(b) MIMO

Figure 1.1: Block diagram of SISO and MIMO systems.

1.1 MIMO Wireless Communications

In a conventional radio system, one transmit (TX) antenna and one receive (RX) antenna is used for transmission of information over a communication channel, which is why it is known as a single-input single-output (SISO) system. The block diagram of such a SISO system is given in Figure 1.1(a). The channel response in this case can be represented by $h(t, \tau)$, at delay bin τ and time instant t. If the channel can be simplified as being time and frequency invariant, the dependence of t and τ is dropped such that the channel is simply denoted by a scalar h. This is the case for narrow band systems operating in a static environment. The sampled scalar signal model is given as

$$y = hx + n, \tag{1.1}$$

where y is the received signal, x is the transmitted signal, and n is characterized by additive white Gaussian noise (AWGN) with zero mean and variance σ_{n}^2. In a noise-limited scenario, the spectrum efficiency of a channel is upper bounded by the Shannon capacity expressed in terms of bits per second per Hertz (bps/Hz), as

$$C = \log_2 \left(1 + \frac{P_{\mathrm{T}}}{\sigma_{\mathrm{n}}^2} |h|^2 \right), \tag{1.2}$$

where P_{T} denotes the transmit power, and $|h|^2$ denotes the power gain of the scalar channel. The expression in (1.2) indicates that channel capacity only increases logarithmically with an increase in transmit power, *e.g.*, at high signal-to-noise ratios (SNRs) or $P_{\mathrm{T}} \gg \sigma_{\mathrm{n}}^2$, a 3 dB increase (or doubling) of the power would only yield 1 extra bps/Hz. This indicates that the performance of a wireless communication system is constrained by either power-limited operation

or bandwidth-limited operation. Given a frequency bandwidth, the use of multiple antennas can improve the spectrum efficiency of the system.

As sketched in Figure 1.1(b), a MIMO system makes use of multiple antenna elements at both TX and RX ends. The channel response is now denoted by a channel matrix $\mathbf{H}$, whose (k,l)-th element $h_{k,l}$ denotes the scalar SISO channel between the k-th RX antenna and the l-th TX antenna. In this case, the sampled vector signal model is given as

$$\boldsymbol{y} = \mathbf{H}\boldsymbol{x} + \boldsymbol{n}, \tag{1.3}$$

where $\boldsymbol{y}$ is the received signal vector at the M_{R} receive antennas, $\boldsymbol{x}$ is the transmitted signal vector for the M_{T} transmit antennas, and $\boldsymbol{n}$ is the AWGN vector at the M_{R} receive antennas. The study of such a system has been the subject of several pioneering works [5–7]. The capacity of an instantaneous MIMO channel can be calculated as

$$C = \log_2 \det\left(\mathbf{I}_{M_{\mathrm{R}}} + \frac{P_{\mathrm{T}}}{M_{\mathrm{T}}\sigma_{\mathrm{n}}^2}\mathbf{H}\mathbf{H}^H\right), \tag{1.4}$$

where $\mathbf{I}_{M_{\mathrm{R}}}$ is a $M_{\mathrm{R}} \times M_{\mathrm{R}}$ identity matrix, $\det(\bullet)$ is the determinant operator, and $(\bullet)^H$ denotes the conjugate transpose (or Hermitian) operator. In this expression, the transmit power P_{T} is assumed to be equally allocated over the M_{T} transmit antennas, corresponding to the case of no channel state information (CSI) at the transmitter. Power allocation can be optimized using a waterfilling algorithm, if the CSI is available at the transmitter. Assuming that the channels for all pairs of RX and TX antennas are mutually uncorrelated independent and identically distributed (IID) complex Gaussian random variables, the mathematical formulation in [7] shows that the MIMO channel offers a $\min(M_{\mathrm{R}}, M_{\mathrm{T}})$-fold increase in capacity comparing to that of the SISO channel, where the operator $\min(M_{\mathrm{R}}, M_{\mathrm{T}})$ picks the smaller value between the number of TX/RX antennas.

This increase is significant since the spectrum efficiency becomes linearly proportional to the number of antennas. In Figure 1.2, the impact of MIMO systems on spectrum efficiency is illustrated with the tradeoff between the required bandwidth (BW) and the number of antennas in achieving a target date rate of 1 Gbps. For example, if we assume a 20 dB SNR in a SISO system as denoted by $\rho = P_{\mathrm{T}}/\sigma_{\mathrm{n}}^2$, one needs to occupy a frequency bandwidth of $BW = 150$ MHz. Therefore, this requirement constrains the system performance in bandwidth-limited operations. On the other hand, for the same SNR, assuming a MIMO system of $M_{\mathrm{R}} = M_{\mathrm{T}} = 6$, the occupied bandwidth can theoretically be reduced to 30 MHz, if the aforementioned IID channel is assumed. This simple example demonstrates the effectiveness of MIMO technology in

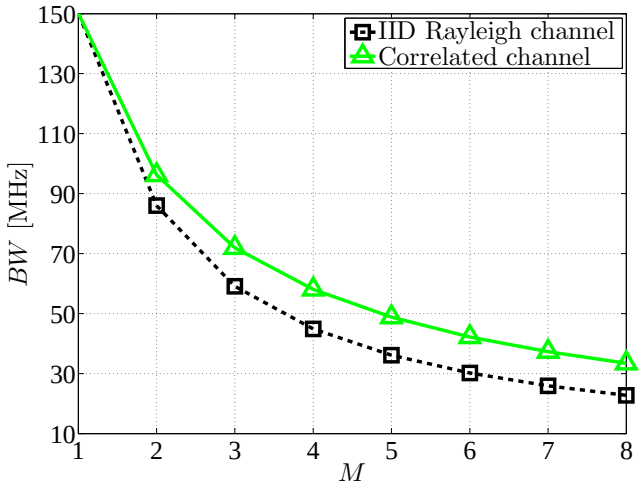

Figure 1.2: Tradeoff in required bandwidth BW and number of antennas (M) in achieving 1 Gbps for a $M \times M$ MIMO channel with 20 dB SNR.

drastically improving spectrum efficiency, which is especially beneficial due to the frequency spectrum being a scarce and expensive resource today. However, real wireless propagations are often more complicated than what the IID model predicts. For example, Figure 1.2 also shows that if there are some correlations among the channel coefficients, the occupied frequency bandwidth is now increased to 42 MHz for the six-antenna case. The rationale behind introducing channel correlation and choosing of six transmit and receive antennas in this simple example will be revealed in the following parts of this thesis.

1.1.1 Propagation Channel

As mentioned above, the ability to unleash the full potential of MIMO systems relies on the properties of the overall propagation channel $\mathbf{H}$, which includes the impacts of the TX and RX multi-antenna systems. Characteristics of MIMO channels will be addressed here, following which some useful channel models will be summarized.

Multi-path Propagation

In free space, electromagnetic waves that are launched from the TX antenna reach the RX antenna along the line-of-sight (LOS) propagation path. However, in mobile communications, the key propagation mechanism is non-LOS (NLOS) multi-path propagation [8]. This is mainly caused by the interaction of radio waves with different types of scattering objects in the radio channel. For example, the transmitted radio waves can be shadowed by large objects, reflected from smooth surfaces, scattered from rough surfaces, and diffracted at the edges of these scatterers. The received signal is therefore a summation of multiple copies of the transmitted signal that travel through these different propagation paths, known as multi-path components (MPCs). These MPCs add constructively and destructively, causing the multi-path fading phenomenon. In a SISO system, one needs to design dedicated transceiver algorithms (*e.g.*, equalization) in order to combat performance degradation due to multi-path fading. However, multi-path fading turns out to be the key for utilizing multi-antenna techniques. For instance, there is a significantly smaller probability that all the signals across spatially separated antennas experience deep fade simultaneously, as compared to it occurring in the signal from one antenna. The approaches that exploit this aspect of multi-antenna systems are known as space diversity techniques.

NLOS/LOS

In a NLOS scenario, there are a large number of scatterers that cause multi-path propagation, but there is no dominant path. In a SISO channel, the complex-valued baseband representation [9] of the channel response h can be modeled as a zero mean complex Gaussian variable with variance σ_0^2, *i.e.*,

$$h \sim \mathcal{CN}(0, \sigma_0^2). \tag{1.5}$$

Equivalently, $\mathrm{Re}\{h\}$ and $\mathrm{Im}\{h\}$ are IID variables of the real-valued Gaussian (or normal) distribution $\mathcal{N}(0, \sigma_0^2/2)$, where $\mathrm{Re}\{h\}$ and $\mathrm{Im}\{h\}$ denote the real and imaginary parts of h. In this case, the amplitude $|h|$ is Rayleigh distributed and the phase φ is uniformly distributed between 0 and 2π [8].

On the other hand, when a dominant path of amplitude A_0 exists among the MPCs, the fading channel is best modeled using a Rician distribution. The scenario is commonly referred to as LOS, although the dominant component does not necessarily propagate along the line-of-sight path. In order to characterize the significance of the dominant component, the Rician K-factor is defined as the ratio of the power in the dominant component to the power in

the scattered components [8], *i.e.*,

$$K = \frac{A_0^2}{2\sigma_0^2}. \tag{1.6}$$

If the dominant component does not exist, *i.e.*, $K \to 0$, the Rician distribution reduces to the Rayleigh distribution. Other distributions, which can better describe some scenarios, are also found in the literature [10]. The IID Gaussian model used in the mathematical formulation of [7] assumes that each element of the channel matrix $\mathbf{H}$ is an IID variable of $\mathcal{CN}(0, \sigma_0^2)$. Therefore, such a $\mathbf{H}$ matrix is referred to as the IID Rayleigh MIMO channel. The rows or columns of such a channel matrix are linearly independent, which ensures that the channel matrix is full rank. The full rank condition of the channel in NLOS scenario is favorable for MIMO systems. On the other hand, the dominant component in the LOS scenario can impair this condition by causing the condition number of $\mathbf{H}$ to increase, due to large amount of power being available to only one subchannel (*i.e.*, the dominant path).

Correlation

Although it has not yet been discussed in great detail as to why the IID Rayleigh MIMO channel is desirable, the author would like to point out at this point that in reality, correlations do often exist among the elements of the channel matrix $\mathbf{H}$. The following example investigates the correlation among the received signals from spatially separated antennas in random propagation channels.

An antenna is characterized by its far-field radiation pattern, with the gain pattern denoted by

$$G_{\theta,\phi}(\Omega) = |E_{\theta,\phi}(\Omega)|^2, \tag{1.7}$$

where $E_{\theta,\phi}(\Omega) = E_\theta(\Omega)\hat{\theta} + E_\phi(\Omega)\hat{\phi}$ includes both θ- and ϕ-polarization components of the complex-valued electric far-field pattern at the solid angle Ω. On the other hand, the propagation channel is characterized by the incident field of the RX antenna system. This can be described by a distribution of the angular power spectrum (APS)

$$P_{\theta,\phi}(\Omega) = P_\theta(\Omega)\hat{\theta} + P_\phi(\Omega)\hat{\phi}, \tag{1.8}$$

where $P_\theta(\Omega)$ and $P_\phi(\Omega)$ denote the θ- and ϕ-polarization components of the incident field, respectively. The power ratio between the two polarizations is denoted as cross-polarization discrimination (XPD), *i.e.*,

$$\chi = \frac{P_{\mathrm{T},\theta}}{P_{\mathrm{T},\phi}}, \tag{1.9}$$

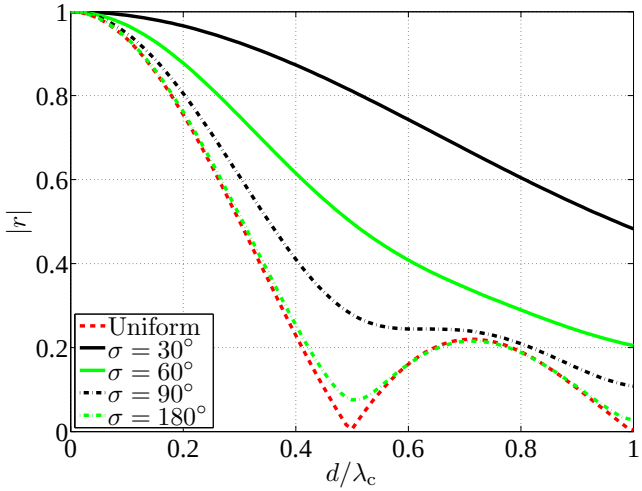

Figure 1.3: Correlation of two isotropic antenna elements separated by distance d in uniform 3D and Gaussian 3D APS centered at ($\theta_0 = 60°, \phi_0 = 0°$) with $\sigma_\theta = \sigma_\phi = \sigma$.

where $P_{\mathrm{T},\theta}$ and $P_{\mathrm{T},\phi}$ denote the total power of θ- and ϕ-polarized fields, respectively. Given a propagation scenario specified by $P_{\theta,\phi}(\Omega)$, the complex correlation between the k-th and l-th antenna elements can be calculated with the following expression using their radiation patterns as [10]

$$r_{k,l} = \frac{\int \left(\frac{\chi}{1+\chi} E_{\theta,k}(\Omega) E^*_{\theta,l}(\Omega) P_\theta(\Omega) + \frac{1}{1+\chi} E_{\phi,k}(\Omega) E^*_{\phi,l}(\Omega) P_\phi(\Omega) \right) \mathrm{d}\Omega}{\sqrt{G_{\mathrm{e},k}} \sqrt{G_{\mathrm{e},l}}}, \quad (1.10)$$

where $E_{\theta,k}(\Omega)$ and $E_{\phi,k}(\Omega)$ denote θ- and ϕ-polarization components of the far-field pattern for the k-th antenna, and the normalization factor G_e denotes the mean effective gain (MEG) of the antenna [11]. The MEG is used to evaluate the effective gain of the antenna system averaged over a given propagation scenario. For the k-th antenna, it is obtained as

$$G_{\mathrm{e},k} = \int \left(\frac{\chi}{1+\chi} G_{\theta,k}(\Omega) P_\theta(\Omega) + \frac{1}{1+\chi} G_{\phi,k}(\Omega) P_\phi(\Omega) \right) \mathrm{d}\Omega. \quad (1.11)$$

In this example, only isotropic antennas are considered, *i.e.*,

$$G_{\theta,k}(\Omega) = G_{\phi,k}(\Omega) = 1/2. \quad (1.12)$$

For a two-element array, where the antennas are separated by a distance d along the x-axis of the coordinate system, ignoring mutual coupling between the antenna elements, the relative array response is obtained using the array factor [12], *i.e.*,

$$E_2(\theta,\phi) = E_1(\theta,\phi)\exp\left[j2\pi\frac{d}{\lambda_c}\sin\theta\cos\phi\right], \tag{1.13}$$

where λ_c denotes the wavelength of the operating frequency f_c, θ and ϕ denote the elevation and azimuth angles, respectively. In order to study the correlation of such a two-element antenna system, two different distributions of APS are considered in this example. First, as a reference scenario, a uniform 3D distribution is used to model a completely random environment, where

$$P_{\theta,\phi}^{\text{Uniform}}(\Omega) \propto 1. \tag{1.14}$$

The second case considers a (truncated) Gaussian distribution, which is a statistically appealing form for APS [10], given by

$$P_{\theta,\phi}^{\text{Gaussian}}(\theta,\phi) \propto \exp\left[-\left(\frac{(\theta-\theta_0)^2}{2\sigma_\theta^2}+\frac{(\phi-\phi_0)^2}{2\sigma_\phi^2}\right)\right], \tag{1.15}$$

where the mean angle-of-arrival (AOA) is denoted as (θ_0,ϕ_0), and the standard deviation of the angular spread is given by $(\sigma_\theta,\sigma_\phi)$. The discussion can easily be extended to the use of a Laplacian distribution, which is found to be a better model of the APS in some scenarios [10].

For the completely random uniform 3D environment described by $P_{\theta,\phi}^{\text{Uniform}}$, the correlation coefficient is given by a sinc function as

$$r(d) = \text{sinc}(k_c d) = \frac{\sin(k_c d)}{k_c d}, \tag{1.16}$$

where the wavenumber $k_c = 2\pi/\lambda_c$. The first zero-crossing point is obtained with the antenna separation of $d = \lambda_c/2$ as shown in Figure 1.3. In other words, two antennas need to be separated by half a wavelength in order to obtain full decorrelation. For the Gaussian distributed APS, a closed form expression for calculating the correlation coefficient is obtained in [13] for the azimuth-only 2D scenario. The correlation for the more general 3D case can be evaluated numerically using (1.10). For example, Figure 1.3 also evaluates the magnitude of the correlation coefficient $|r|$ of the two-element isotropic antenna array denoted by (1.13) under the Gaussian APS with different angular spreads. The APS is centered at the AOA direction of $(\theta_0 = 60^\circ, \phi_0 = 0^\circ)$,

which is an elevated angle in the end-fire direction of the array [12]. For APS with smaller angular spreads, it can be seen that larger separation distances are required in order to obtain reasonably low correlation of $|r| < 0.7$, which is roughly equivalent to the envelope correlation of less than 0.5. The performance converges to that of the uniform 3D distribution when the angular spread is large enough.

The study illustrates that a multi-antenna system can be exposed to severe spatial correlation if the interaction between the antennas and the propagation channel is not properly exploited. It also suggests the need of other techniques for obtaining linearly independent channels, since it is not always possible to accommodate large spatial separation among antennas in some applications, especially where the size of the overall antenna system is constrained.

Polarization

It has been known that the two polarization states of plane waves can be used to provide two independent communication channels [14, 15]. This mechanism has become particularly interesting since it offers the benefit of allowing two antennas to be closely placed, which is desirable for miniaturizing an antenna system. Recent attempts to measure and model polarized propagation channels are reported in a number of research articles, including [16–21]. In most of these studies, the focus is to model the coupling between co-polarized and cross-polarized radio waves.

Considering dual-polarized antennas at both the TX and RX ends, the 2×2 channel matrix $\mathbf{H}$ is formulated as

$$\mathbf{H} = \begin{bmatrix} h_{\mathrm{VV}} & h_{\mathrm{VH}} \\ h_{\mathrm{HV}} & h_{\mathrm{HH}} \end{bmatrix}, \tag{1.17}$$

where h_{VH} denotes the channel transfer function between the horizontally (H) polarized TX antenna and the vertically (V) polarized RX antenna. Similar notations are applicable to all other TX-RX antenna pairs. One common parameter in characterizing dual-polarized channels is to model the channel's cross-polarization coupling capability. This can be described by the cross-polarization ratio (XPR) as

$$\chi_{\mathrm{V}} = \frac{\mathbb{E}\{|h_{\mathrm{HV}}|^2\}}{\mathbb{E}\{|h_{\mathrm{VV}}|^2\}}, \chi_{\mathrm{H}} = \frac{\mathbb{E}\{|h_{\mathrm{VH}}|^2\}}{\mathbb{E}\{|h_{\mathrm{HH}}|^2\}}, \tag{1.18}$$

where $\mathbb{E}\{\bullet\}$ denotes the expectation operator. χ_{V} is defined as the power ratio between the cross-polarized coupling from the V-polarized TX antenna to the H-polarized RX antenna and the co-polarized coupling of the V-polarized TX

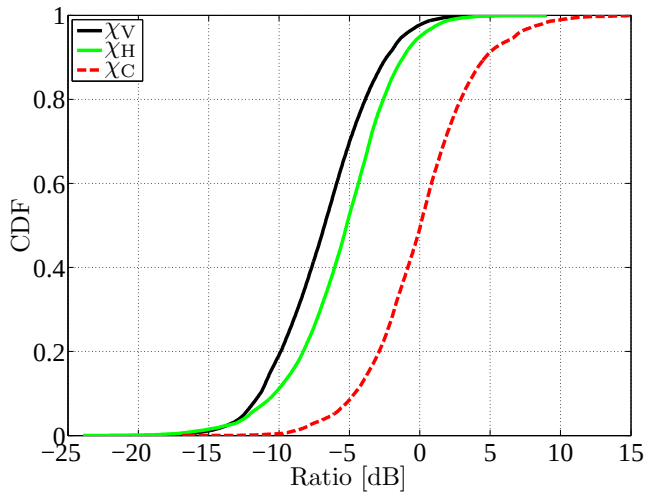

Figure 1.4: The CDFs of co- and cross-polarization ratios for an urban macrocellular dual-polarized channel.

and RX antennas. Similarly, χ_{H} denotes the XPR for the H-polarized TX antenna. The co-polarization ratio (CPR) is also defined in a similar manner, and it describes the power ratio between the co-polarized V-to-V (h_{VV}) and H-to-H (h_{HH}) channels, as

$$\chi_{\mathrm{C}} = \frac{\mathbb{E}\{|h_{\mathrm{VV}}|^2\}}{\mathbb{E}\{|h_{\mathrm{HH}}|^2\}}. \tag{1.19}$$

The cumulative distribution functions (CDFs) of the co- and cross-polarization ratios obtained from a channel sounding measurement in an urban macrocellular propagation scenario is shown in Figure 1.4. At median probability (50%), the CPR is found to be 0 dB, which indicates the quasi equivalent ability of the propagation channel in co-polarization coupling of V- and H-polarized waves. On the other hand, the XPR is found to be lower than −5 dB. Similar to other studies, the result indicates that cross-polarization coupling in such an environment is $5 - 6$ dB weaker than co-polarization coupling.

Analytical Channel Model

Modeling electromagnetic wave propagation in a multi-path environment is a complex problem. However, it is always desired to have accurate yet tractable

channel models. Accurate channel models are crucial for MIMO systems, since the channel matrix $\mathbf{H}$ plays the key role in determining the upper bound of channel capacity as given in (1.4). According to the survey study in [22], different channel models can be classified into analytical and physical models. This thesis focuses on the stochastic approach in studying these two classes of channel models.

The analytical approach models the channel without considering the underlying physical aspects. The simplest and most important channel model is the IID Rayleigh MIMO channel that has been discussed previously. Denoting it as $\mathbf{H}_{\mathrm{IID}}$, the matrix elements $h_{k,l} = [\mathbf{H}_{\mathrm{IID}}]_{k,l}$ are IID complex Gaussian random variables with unit variance $\mathcal{CN}(0,1)$, *i.e.*,

$$\mathbb{E}\{h_{k,l}\} = 0, \mathbb{E}\{|h_{k,l}|^2\} = 1, \mathbb{E}\{h_{k,l}h^*_{m,n}\} = 0, \tag{1.20}$$

where $\{\bullet\}^*$ denotes the complex conjugate operator. The squared Frobenius norm of $\mathbf{H}_{\mathrm{IID}}$ is therefore given by

$$\mathbb{E}\left\{||\mathbf{H}_{\mathrm{IID}}||_{\mathrm{F}}^2\right\} = \mathbb{E}\left\{\sum_{k=1}^{M_{\mathrm{R}}}\sum_{l=1}^{M_{\mathrm{T}}}|h_{k,l}|^2\right\} = M_{\mathrm{R}}M_{\mathrm{T}}. \tag{1.21}$$

The quantity $||\mathbf{H}||_{\mathrm{F}}^2$ represents the total power gain of the channel matrix. Since the MIMO channel capacity depends on the SNR and as well as the channel gain, the channel matrix is usually normalized according to (1.21) in order to interpret the results correctly [23]. $||\mathbf{H}||_{\mathrm{F}}^2$ can also be expressed as

$$||\mathbf{H}||_{\mathrm{F}}^2 = \mathrm{Tr}\left(\mathbf{H}\mathbf{H}^H\right) = \sum_{k=1}^{\kappa}\lambda_k, \tag{1.22}$$

where $\{\mathrm{Tr}(\bullet)\}$ denotes the trace operator, λ_k $(k = 1, 2, \ldots, \kappa)$ are the non-zero eigenvalues of $\mathbf{H}\mathbf{H}^H$, and κ denotes the rank of the matrix. The eigenvalues can be obtained using eigenvalue decomposition, *i.e.*,

$$\mathbf{H}\mathbf{H}^H = \mathbf{Q}\Lambda\mathbf{Q}^H, \tag{1.23}$$

where $\Lambda = \mathrm{diag}\left[\lambda_1, \lambda_2, \ldots, \lambda_{M_{\mathrm{R}}}\right]$ in the case of a full rank matrix with $\kappa = M_{\mathrm{R}}$.

In order to include spatial correlation properties into the channel model, the Kronecker model is proposed to introduce the correlation at the TX and RX ends separately. The composed channel matrix is given by [24]

$$\mathbf{H}_{\mathrm{K}} = \mathbf{R}_{\mathrm{RX}}^{1/2}\mathbf{H}_{\mathrm{IID}}(\mathbf{R}_{\mathrm{TX}}^{1/2})^T, \tag{1.24}$$

where $(\bullet)^T$ denotes the transpose operator, $\mathbf{R}_{\mathrm{RX}}$ and $\mathbf{R}_{\mathrm{TX}}$ denotes the correlation matrix of the RX and TX arrays, respectively. The underlying assumption

made in this model is that the local APS caused by clusters of scatterers exist at the two ends of the channel individually, with no direct link interacting between the two local scattering environments. Although the model has been validated in measurements [25], it is also known that the Kronecker model fails to predict the performance of channels where strong correlation exists between the respective local APS at the TX and RX ends [26].

Either $\mathbf{H}_{\text{IID}}$ or $\mathbf{H}_{\text{K}}$ can be used to represent NLOS scenarios. For LOS scenarios, the Rician K-factor is used to introduce the dominant component, which results in the following LOS channel [24]

$$\mathbf{H}_{\text{LOS}} = \sqrt{\frac{K}{1+K}}\overline{\mathbf{H}} + \sqrt{\frac{1}{1+K}}\mathbf{H}_{\text{IID}}, \tag{1.25}$$

where the dominant component is deterministic and can be described by $\overline{\mathbf{H}} = \mathbb{E}\{\mathbf{H}_{\text{LOS}}\}$. The Rician K-factor represents the ratio between the power of the dominant component and the power of the scattered components as defined in (1.6). With $K \to 0$, the channel matrix becomes the IID Rayleigh channel $\mathbf{H}_{\text{IID}}$. On the other hand, when $K \to \infty$, the channel is fully deterministic, *i.e.*, no fading. Therefore, the performance of the channel under large K values largely depends on the structure of $\overline{\mathbf{H}}$.

In LOS scenario, the structure of $\overline{\mathbf{H}}$ is such that high correlation is often obtained for spatially separated antennas, similar to the cases of narrow angular spreads in Figure 1.3. However, two independent channels can still be exploited using polarization diversity. If dual-polarized antennas are employed at both the TX and RX ends, the eigenvalues of $\overline{\mathbf{H}}$ can become equal, which is a particularly favorable situation for the MIMO technique to be discussed in Section 1.1.2.

Physical Channel Model

In order to account for the physical behavior of multi-path propagation, stochastic channel models can also be studied using a physical approach based on the parameters of MPCs, such as attenuation, delay, polarization, AOA and angle-of-departure (AOD). Utilizing directional information, the radio channel can be separated from the antennas using the double-directional channel concept [27]. The model is described by the statistical distribution of the MPCs parameters based on rays and clusters of rays (of plane waves). An alternative approach makes use of spherical vector waves to model the MPCs, which allows the interaction between the channel and the antennas to be studied in the spherical wave mode domain [28, 29].

Figure 1.5 illustrates the concept of random scattering channel model, which is similar to the double-bounce stochastic model discussed in [30]. $s_{\text{t}k}$ ($k =$

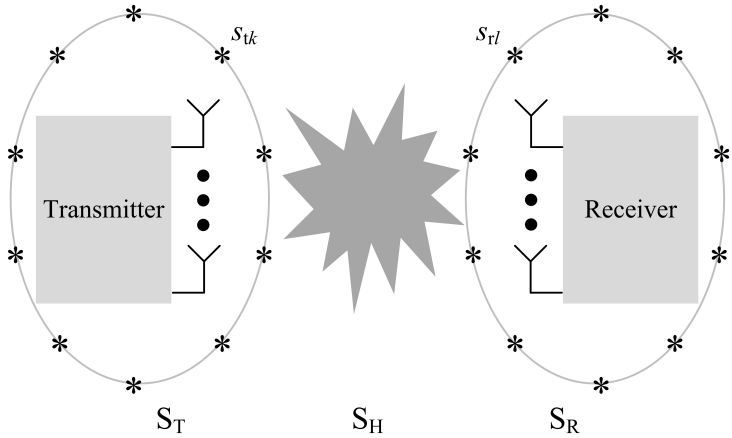

Figure 1.5: Random scattering channel model.

$1, 2, \ldots, M_{\mathrm{ST}}$) represent a number of local clusters of scatterers in the scattering medium surrounding the TX antennas, and s_{rl} ($l = 1, 2, \ldots, M_{\mathrm{SR}}$) represent a number of local clusters of scatterers surrounding the RX antennas. The local scattering matrix of the TX and RX antenna is represented by $\mathbf{S}_{\mathrm{T}}$ and $\mathbf{S}_{\mathrm{R}}$, of size $M_{\mathrm{ST}} \times M_{\mathrm{T}}$ and $M_{\mathrm{R}} \times M_{\mathrm{SR}}$, respectively. The scattering matrix linking the two local scatterers is denoted by $\mathbf{S}_{\mathrm{H}}$, which is of size $M_{\mathrm{SR}} \times M_{\mathrm{ST}}$. The scatterers follow the statistical distribution of the local APS, obtained from either measurements or analytical models. If a completely random scattering environment is considered for $\mathbf{S}_{\mathrm{H}}$, the model is then equivalent to the Kronecker channel model. On the other hand, if only one link exists in $\mathbf{S}_{\mathrm{H}}$, it leads to the degenerated keyhole channel [31].

1.1.2 Space-Time Processing

Advantages of using multiple antennas, either on one end or on both ends of a communication channel, can be seen from several aspects. How these advantages are exploited depends on the applied space-time processing technique [24, 32]. For example, directional radiation patterns can be formed using antenna arrays for spatially-selective transmission and/or reception of signals, which lead to array gain and improved link quality. In a multi-user cellular system, it can also contribute to the mitigation of interference, *e.g.*, the base station (BS) antenna array can form a null in the array pattern towards the direction of the interfering user. Another common space-time processing technique is antenna diversity. In the case of RX diversity, the received signal from

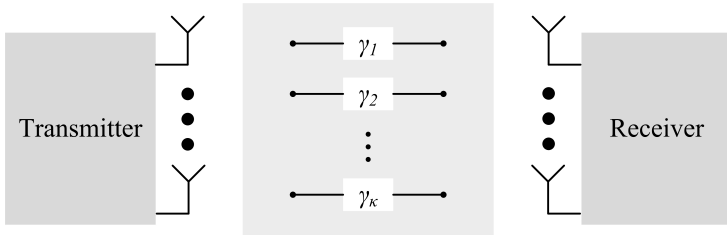

Figure 1.6: Eigenchannel representation of spatial multiplexing scheme.

different multiple antennas may be fading independently. Given the knowledge of the channel, the received signals can be combined constructively. Diversity can also be exploited at the TX side in the absence of channel knowledge by means of space-time coding. Antenna diversity techniques have been studied over several decades, and one current focus is on their implementation in compact user terminals [33].

In this thesis, the discussion of MIMO systems focuses on the spatial multiplexing technique, which offers the potential of parallel information transmission to achieve a capacity that is linearly proportional to the number of antennas.

Spatial Multiplexing

In the spatial multiplexing technique, multiple streams of information can be transmitted in parallel between multiple TX and RX antennas. A transceiver architecture that applies the spatial multiplexing scheme is proposed in [34]. In order to show that the spatial multiplexing technique can achieve a MIMO capacity that is linearly proportional to the number of antennas, the channel matrix $\mathbf{H}$ plays the key role. Applying the eigenvalue decomposition of $\mathbf{H}\mathbf{H}^H$ defined in (1.23), the channel capacity in (1.4) becomes

$$C = \sum_{k=1}^{\kappa} \log_2 \left(1 + \frac{P_\mathrm{T}}{M_\mathrm{T}\sigma_\mathrm{n}^2}\lambda_k\right) = \sum_{k=1}^{\kappa} \log_2(1+\gamma_k). \tag{1.26}$$

The expression shows that the capacity of the MIMO channel is the sum capacity of κ scalar eigenchannels. As illustrated in Figure 1.6, each eigenchannel is characterized by its effective channel gain γ_k, which is proportional to the corresponding eigenvalue λ_k, *i.e.*,

$$\gamma_k = \frac{P_\mathrm{T}}{M_\mathrm{T}\sigma_\mathrm{n}^2}\lambda_k = \frac{\rho}{M_\mathrm{T}}\lambda_k, k = 1, 2, \ldots, \kappa, \tag{1.27}$$

where as before $\rho = P_{\mathrm{T}}/\sigma_{\mathrm{n}}^2$ is the SNR. In order to access the parallel eigenchannels, the knowledge of $\mathbf{H}$ needs to be available at both the TX and RX ends. Applying singular value decomposition to $\mathbf{H}$ together with appropriate pre- and post-processing of the transmitted and received signals, the sampled vector channel model of MIMO system in (1.3) can be shown to become a set of κ parallel scalar SISO channels [24], given as

$$\tilde{y}_k = \sqrt{\lambda_k}\tilde{x}_k + \tilde{n}_k, k = 1, 2, \ldots, \kappa. \tag{1.28}$$

Each of the parallel channels is characterized by its associated eigenvalue. Considering the special case with a square channel matrix of full rank, with $\kappa = M = M_{\mathrm{R}} = M_{\mathrm{T}}$ and having identical eigenvalues, if the channel matrix has been normalized according to (1.21), using (1.22), the eigenvalues are given as

$$\lambda_k = M, k = 1, 2, \ldots, M. \tag{1.29}$$

The effective eigenchannel gain γ_k defined in (1.27) is then equal to the SISO SNR ρ. Therefore, the channel capacity in (1.26) becomes exactly M-fold of the SISO channel capacity, *i.e.*,

$$C = M \log_2(1 + \rho). \tag{1.30}$$

As is explained above, identical eigenvalues are desired. In fact, it can be shown that, given a fixed total channel gain (1.22), the distribution of eigenvalues which maximizes capacity corresponds to equal gain across the eigenvalues. One way to characterize the departure from this ideal behavior is to evaluate the "flatness" or dispersion across the eigenvalues, which is calculated as the ratio between the geometric mean and the arithmetic mean of eigenvalues, *i.e.*,

$$\frac{(\prod_{k=1}^{\kappa} \lambda_k)^{1/\kappa}}{\frac{1}{\kappa}\sum_{k=1}^{\kappa} \lambda_k}. \tag{1.31}$$

This metric is also known as ellipticity statistics. In [35], it is demonstrated that a higher eigenvalue dispersion of the measured channel can be interpreted as a degradation in SNR.

However, from the viewpoint of the propagation channel, having identical channel eigenvalues is only possible in very specific channels [36]. For example, this is the case in LOS scenario when both V- and H-polarized waves are exploited in the 2×2 MIMO channel matrix, *i.e.*, $\overline{\mathbf{H}} \propto \mathbf{I}_2$ and $K \to \infty$ in (1.25). In more general cases, although the sum of all eigenvalues is bounded as in (1.22), the strengths of each individual eigenvalues are spread over a range of values. For the IID Rayleigh MIMO channel with many antenna elements, a

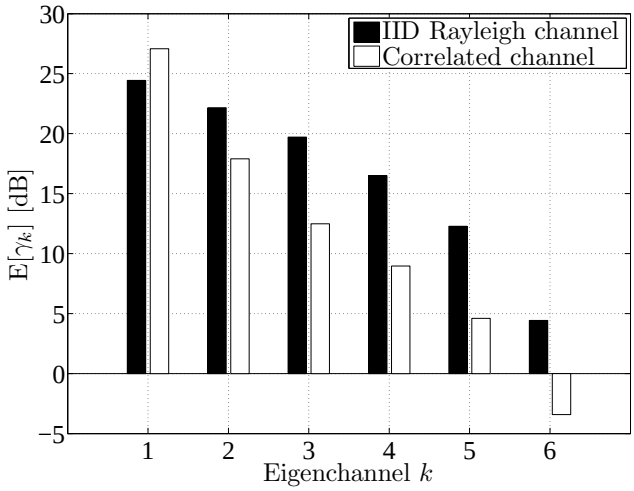

Figure 1.7: Effective eigenchannel gain γ_k of the 6×6 MIMO channel with 20 dB SNR.

statistical distribution of all the eigenvalues can be obtained using the random matrix theory [37].

In this thesis, the discussion is mainly focused on 6×6 MIMO systems. In Figure 1.7, the mean values of the effective eigenchannel gains γ_k of the 6×6 IID Rayleigh MIMO channels with 20 dB SNR are shown. As can be seen, the gains are spread over the eigenchannels, with the strongest and weakest channel gains differing by 20 dB. For the given SNR, six parallel channels can be supported using spatial multiplexing, since the weakest channel still yields a modest gain (or in effect, SNR) of just under 5 dB. If channel knowledge is available at the transmitter, the waterfilling algorithm can be applied here to improve the capacity. However, in a correlated channel where a correlation coefficient of $|r| = 0.7$ is assumed between all pairs of TX and RX antennas, the weakest channel gain is found to be lower than 0 dB (see Figure 1.7). This indicates that not all eigenchannels can be efficiently utilized in parallel. The concept of effective degrees-of-freedom (EDOF) is proposed in [38] to quantify the number of eigenchannels that can be efficiently exploited for spatial multiplexing. For a given SNR ρ, the EDOF, denoted as N_{DOF}, is defined as

$$N_{\mathrm{DOF}} = \frac{\mathrm{d}}{\mathrm{d}\delta} C(2^{\delta}\rho)|_{\delta=0}. \tag{1.32}$$

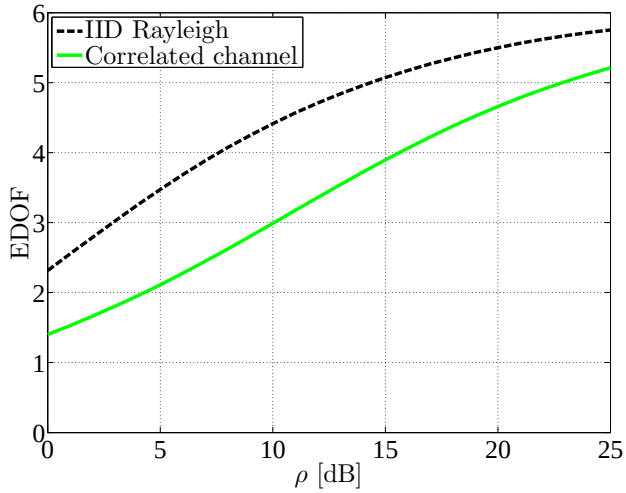

Figure 1.8: Effective DOF of 6×6 MIMO channels.

If the capacity is obtained using (1.26), the EDOF can be calculated as

$$N_{\mathrm{DOF}} = \sum_{k=1}^{\kappa} \frac{1}{1 + M_{\mathrm{T}}/(\rho\lambda_k)} = \sum_{k=1}^{\kappa} \frac{1}{1 + 1/\gamma_k}. \tag{1.33}$$

In Figure 1.8, the EDOF performance of the 6×6 MIMO channel is shown. With a reference SNR of 20 dB, nearly six DOFs are obtained with the IID Rayleigh channel. However, only less than five eigenchannels can be supported in the case of the correlated channel.

1.2 Multi-antenna Systems

From the discussion above, the central role of the propagation channel in studying MIMO systems has been described. The potential of MIMO systems is therefore limited by the propagation channel, and its interaction with the multi-element antennas. This interaction has been briefly addressed in Section 1.1.1 where the correlation across the RX antenna elements is obtained given different distributions of the incident field. This aspect is further investigated in the following sections.

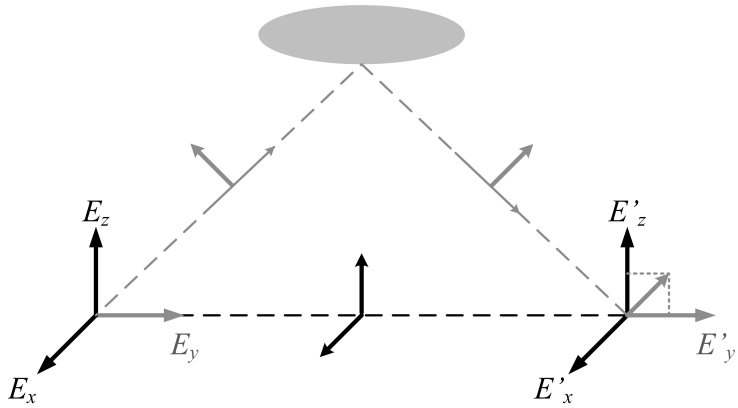

Figure 1.9: The use of three field components of the electric field in the presence of a scatterer [40].

1.2.1 Degree-of-Freedom

A multi-antenna system has the best performance when the correlation among the signals on different antenna branches is low (assuming equal average branch power). In conventional configurations, antenna elements are usually spatially separated. It has been shown above (*e.g.*, Figure 1.3) that a separation distance of at least $d = \lambda_c/2$ is typically required in order to achieve full decorrelation. Even though a reasonably low correlation of $|r| < 0.7$ is considered enough to ensure promising results, it still requires about $\lambda_c/4$ separation in a uniform 3D propagation scenario.

On the other hand, low signal correlation can also be obtained by utilizing polarization diversity, which has the benefit that the antenna elements may be placed very close to one another. In [14], a two-branch polarization diversity system is proposed for the reception of vertically (V) and horizontally (H) polarized electromagnetic waves. The use of two polarization states of the plane waves has been known to introduce two DOFs to a wireless communication channel. This is the case in LOS scenarios, where the transverse propagation of electromagnetic waves are perpendicular to the longitudinal direction of the propagation [39].

For multi-path propagation with scattering object(s), all three components of the electric field may be utilized. This is illustrated in Figure 1.9 [40], where the LOS propagation is along the positive y direction. In this case, three orthogonal electric dipole antennas are assumed for the excitation of the three electric field components, denoted as E_x, E_y and E_z. Without the scatterer,

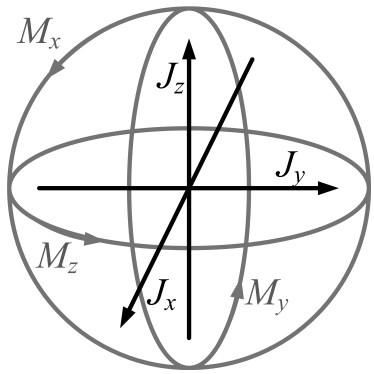

Figure 1.10: Six co-located orthogonally polarized dipoles, where J_x, J_y and J_z denote the electric dipole currents and M_x, M_y and M_z denote the magnetic dipole currents [10].

only E_x and E_z that are perpendicular to the LOS propagation direction can be used. Conventionally, these components are often denoted as H- and V-polarizations, respectively. The third field component E_y that is parallel to the longitudinal direction of the propagation cannot be exploited. With the presence of a scatterer, on the other hand, the radio waves can propagate along a different path. This will lead to a non-zero contribution to E_y. In this way, all three field components are exploited in this two-path propagation environment. This discussion is further addressed in [40] by considering a total of six electric and magnetic field components, *i.e.*, E_x, E_y, E_z, H_x, H_y and H_z. Each component can be excited and received using electric and magnetic dipoles of the corresponding polarization states.

In [40], an array of six co-located and orthogonally polarized electric and magnetic dipole antennas are proposed to transmit and receive six distinguishable field components, each of which can convey information through an independent channel in a rich multi-path scattering environment. The proposed six-element array of electric and magnetic dipole antennas is illustrated in Figure 1.10.

In the context of MIMO systems, an additional three-fold increase in channel capacity can be achieved in addition to the conventional use of two polarizations. In other words, a total number of six DOFs can be exploited. This has attracted considerable interest and sparked further investigation on the number of DOFs that is theoretically available in a wireless channel [28,41–45]. However, the claim regarding the dependence between electric and magnetic fields also leads to some misunderstandings. In fact, as pointed out in [42], the

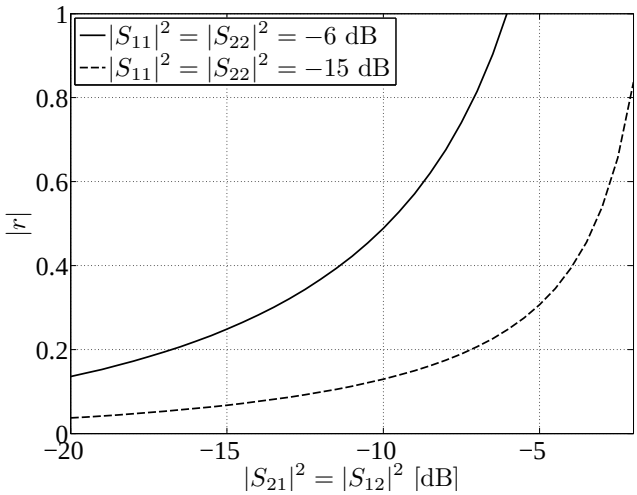

Figure 1.11: Correlation using S-parameter representation.

availability of the six DOFs is better explained in terms of polarization and angle diversities of the multi-element antenna patterns. This is the subject of [46, 47], which are the included Papers I and II in this thesis. The work is further expanded in Chapter 2.

1.2.2 Antenna-Channel Matching

When multiple antenna elements are closely placed with one another, there are strong electromagnetic interactions among the antenna elements. This phenomenon is known as mutual coupling, whose impact on the performance of antenna systems is commonly ignored by many studies. This is especially the case in communication and signal processing communities, which favor simpler models of the array elements. However, since strong coupling can lead to not only high correlation but also severe loss in efficiency of multi-antenna systems, it is important to properly account for coupling in the multi-antenna model [33, 48, 49]. The study of mutual coupling is usually performed using the scattering (S) parameters in a network representation [50–52]. Considering a uniform 3D propagation environment, the correlation of a two-antenna system can be obtained using the two-port S parameter representation as [53, 54]

$$r = -\frac{S_{11}S_{12}^* + S_{21}S_{22}^*}{\sqrt{(1-|S_{11}|^2-|S_{21}|^2)(1-|S_{22}|^2-|S_{12}|^2)}}. \tag{1.34}$$

The correlation coefficient calculated using (1.34) is studied in Figure 1.11, where $S_{11} = S_{22}$ denotes the reflection coefficients and $S_{12} = S_{21}$ denotes the coupling coefficients of the two-port network. It is clear from Figure 1.11 that higher coupling coefficients lead to higher magnitudes of correlation, although in general the antenna efficiencies also play a key role in determining the correlation. For example, the same level of the coupling coefficient leads to higher correlation in the case of higher mismatch loss. In the above discussion, the radiation efficiencies of the antennas are assumed to be 100%, *i.e.*, the antennas are lossless. Detailed discussions on the significance of the radiation efficiency can be found in [54].

Recent work has shown that impedance matching networks can be used to counteract the negative impacts of mutual coupling. For example, optimal performance on signal correlation [55], diversity [50] and capacity [51] can be achieved at the cost of narrower bandwidth [52], if a sophisticated multi-port matching network is utilized. In order to study the impact of matching networks on the performance of multi-antenna systems, we can employ the following system model that is based on the Z-parameter representation. The system model for the RX subsystem is illustrated in Figure 1.12. It consists of the coupled RX antennas, a coupled matching network, and load impedances (or termination). It is noted that this simple model does not take into account noise coupling, which can have a significant impact on the system performance [56, 57]. In Figure 1.12, $\mathbf{Z}_{\mathrm{RR}}$ is a $M \times M$ antenna impedance matrix whose diagonal and off-diagonal elements represent self and mutual impedances, respectively. $Z_{\mathrm{L}m}$ $(m = 1, 2, \ldots, M)$ are the load impedances for the m-th port. The matching network is denoted by $\mathbf{Z}_{\mathrm{M}}$, which represents a $2M \times 2M$ network of the matrix structure

$$\mathbf{Z}_{\mathrm{M}} = \begin{bmatrix} \mathbf{Z}_{11} & \mathbf{Z}_{12} \\ \mathbf{Z}_{21} & \mathbf{Z}_{22} \end{bmatrix}. \tag{1.35}$$

In the RX subsystem above, the excitation sources are the open-circuit voltages $\boldsymbol{V}_{\mathrm{oc}} = [V_{\mathrm{oc}1}, \ldots, V_{\mathrm{oc}M}]^T$. The currents induced at the input of the matching networks $\boldsymbol{I}_{\mathrm{L}} = [I_{\mathrm{L}1}, \ldots, I_{\mathrm{L}M}]^T$ can be obtained as

$$\boldsymbol{I}_{\mathrm{L}} = (\mathbf{Z}_{\mathrm{RR}} + \mathbf{Z}_{\mathrm{ThL}})^{-1} \boldsymbol{V}_{\mathrm{oc}}, \tag{1.36}$$

where $\mathbf{Z}_{\mathrm{ThL}}$ denotes the Thevenin equivalent load impedance as seen by the antenna ports, and it is given by

$$\mathbf{Z}_{\mathrm{ThL}} = \mathbf{Z}_{11} - \mathbf{Z}_{12}(\mathbf{Z}_{\mathrm{L}} + \mathbf{Z}_{22})^{-1}\mathbf{Z}_{21}. \tag{1.37}$$

The output voltages over the load impedances are then found as

$$\boldsymbol{V}'_{\mathrm{L}} = \mathbf{Z}_{\mathrm{L}}\boldsymbol{I}'_{\mathrm{L}} = \mathbf{Z}_{\mathrm{L}}(\mathbf{Z}_{22} + \mathbf{Z}_{\mathrm{L}})^{-1}\mathbf{Z}_{21}\boldsymbol{I}_{\mathrm{L}}. \tag{1.38}$$

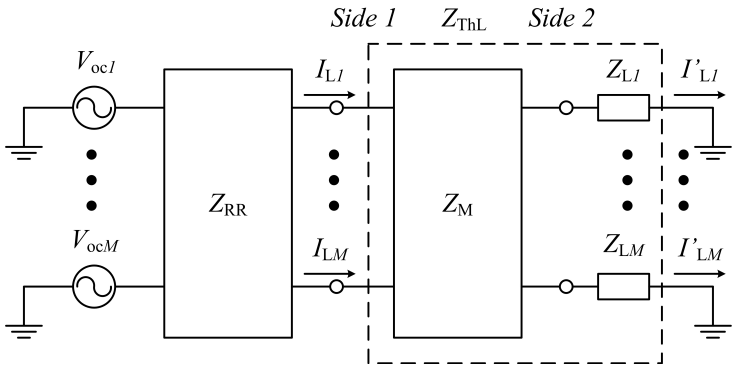

Figure 1.12: Block diagram of a M-antenna RX subsystem.

Substituting (1.36) into (1.38) gives the transfer function between the open-circuit voltages and the output voltages,

$$\boldsymbol{V}'_{\mathrm{L}} = \mathbf{Z}_{\mathrm{L}}(\mathbf{Z}_{22} + \mathbf{Z}_{\mathrm{L}})^{-1}\mathbf{Z}_{21}(\mathbf{Z}_{\mathrm{RR}} + \mathbf{Z}_{\mathrm{ThL}})^{-1}\boldsymbol{V}_{\mathrm{oc}}. \tag{1.39}$$

The relationship between the open-circuit voltages at the RX antenna system and the excitation current at the TX antenna system can be characterized by a trans-impedance channel function, which can be formulated using a path-based channel model [51]. A similar derivation applies in getting the excitation currents across the TX antennas from the signal sources. Thus, a complete system model including the matching network at the RX end can be derived.

The system model above can be applied to optimize the impedance matching networks of multi-antenna systems. Several different matching conditions have been discussed extensively in [50–52, 55], including the characteristic impedance match, self impedance match, input impedance match and multi-port conjugate match. Among these configurations, the uncoupled input impedance matching network exhibits a good balance between performance and complexity, provided that the antenna spacing is not too small (*e.g.*, below $0.05\lambda_{\mathrm{c}}$).

In practice, the optimal matching solution should not only account for the antennas, but also the user in proximity and the propagation channel, *i.e.*, the matching should optimize the antenna-channel interaction. In [58], a method is proposed for determining antenna radiation characteristics that maximize the diversity gain, given the propagation channel, though no user interaction is considered. Practical implementations of adaptive impedance matching networks in realistic multi-antenna terminals is currently an active research topic, see *e.g.*, [59]. In [60, 61], it is found out that the optimized uncoupled impedance

matching networks adapt the array patterns according to the prevailing propagation environment. Depending on the antenna array configuration and the propagation channel, the difference in optimal performance can be significant. This is the subject of [61], which is the included Paper III in this thesis.

1.3 MIMO Cellular Systems

So far, the thesis has only introduced point-to-point MIMO systems, *i.e.*, single-user scenario. In cellular systems, multi-user scenario should be addressed. For example, the downlink case of the cellular system can be studied by considering multiple RX antennas that are spatially distributed over a large geographical area, each of which represents one user with one RX antenna.

Space division multiple access (SDMA) has been known as a radio access network technology that uses multi-antenna systems to allow more than one user in a cell to communicate with the BS on the same frequency and the same time slot [8]. This is because the multi-antenna system used at the BS can distinguish among the users by means of their individual spatial signatures. It can also form a beam for a dedicated user in order to improve link quality, as well as a null to other users in order to suppress co-channel interference. Therefore, the aforementioned space-time processing techniques such as beamforming, diversity and spatial multiplexing can also be exploited to efficiently improve end user performance. In the multiple access channel (MAC), *i.e.*, the uplink case, the capacity region with either independent or joint decoding at the receiver (*i.e.*, the BS) is similar in form to point-to-point capacity with no channel knowledge at the transmitter. This is due to cooperation being possible at the receiver end. However, in this case, the sum rates for all possible combinations of the users (together with their corresponding MAC channels) must be calculated in order to fully define the capacity region. For example, in a two-user case, the capacity region is defined by the individual rates of users 1 and 2 (*i.e.*, R_1 and R_2) as well as the sum rate of the two users, $R_1 + R_2$. In addition, the SNR of each user depends on its own available transmit power, and no sharing of transmit power can occur among the users. In the broadcast channel (BC), a precoding technique known as dirty paper coding (DPC) [62] is recently found to achieve the downlink capacity. There also exists an interesting duality between the uplink and the downlink capacity performances [32].

Along with the evolution of cellular systems, it is becoming increasingly important to not only achieve higher peak data rate, but also higher rates over the entire coverage area. Particularly, for the LTE-Advanced standard, an important goal is to further improve throughput performance at cell edges. In this context, the concept of cooperative MIMO has been proposed, where

antennas of the serving sector/cell as well as the neighboring sectors/cells can work collaboratively. This concept, popularly known as coordinated multi-point (CoMP) transmission and reception, has in fact been introduced as a candidate technique in LTE-Advanced to improve system efficiency and coverage. The CoMP system can be implemented among several BSs (intersite) or within several sectors of a single BS (intrasite) [63]. Using advanced space-time processing techniques, the multi-antenna systems of multiple sectors/cells can cooperate to mitigate the interference and further improve the spectrum efficiency. Thus far, intersite cooperative MIMO has received significant attention in the literature [64–66]. Using largely separated distributed antenna systems (DASs), improved capacity performance has been achieved with intersite CoMP due to reduced correlation, increased SNR because of more frequent LOS scenarios, and shadowing diversity. Intersite cooperation is also known to enhance the rank of the compound channel matrix, hence offering a better capacity performance.

On the other hand, intrasite multi-sector cooperation requires less complexity due to different multi-antenna systems being located within a single BS site. However, the potential performance enhancement using intrasite CoMP is not well explored. A recent study in [63] shows that the cooperation performance can be underestimated using an existing channel model. In [67], the MIMO capacity improvement that can be provided by the intrasite multi-sector cooperation is studied in a measured urban environment. The results show that higher than 40% capacity improvement is achieved at the sector edge region, relative to that of the single-sector link with no cooperation. This work is included as Paper V in this thesis.

Chapter 2

Six-port MIMO Antennas

It has been discussed in Section 1.2.1 that six DOFs can be theoretically exploited in a wireless channel with rich multi-path scattering by using six-element arrays of co-located electric and magnetic dipoles [40]. In this chapter, this topic is discussed in more details. Section 2.1 is dedicated to an analytical study where the results are obtained by simulations. The experimental implementation of the six-element arrays that are able to realize the full six DOFs is discussed in Section 2.2.

2.1 Analytical Study

In [40], the proposed multi-antenna system with six co-located, orthogonally polarized, ideal electric and magnetic (E/M) dipoles has been postulated to be capable of achieving six eigenchannels in the context of MIMO systems. A sketch of the array configuration was provided earlier in Figure 1.10, where J_x, J_y and J_z denote the electric dipole currents and M_x, M_y and M_z denote the magnetic dipole currents for exciting (or sampling) the six electromagnetic field components, E_x, E_y, E_z and H_x, H_y, H_z, respectively. Each magnetic dipole is realized using a loop with uniform current distribution. Similarly, the electric dipoles are ideally infinitesimal dipoles and hence the current is uniform along the length of the dipole. The elements in this array configuration are also known as electromagnetic energy density sensors [10]. Their electric far-field patterns are summarized in Table 2.1.

The analytical study in [42] shows that the array is capable of achieving the ultimate six communication modes in a propagation channel with uniform 3D APS. The availability of six DOFs is explained in terms of polarization and

Table 2.1: Far-field patterns of the electromagnetic energy density sensors [10].

Dipole current	Field component	Electric far-field patterns	
		$E_\theta(\theta,\phi)$	$E_\phi(\theta,\phi)$
J_x	E_x	$\cos\theta\cos\phi$	$-\sin\phi$
J_y	E_y	$\cos\theta\sin\phi$	$\cos\phi$
J_z	E_z	$-\sin\theta$	0
M_x	H_x	$\sin\phi$	$\cos\theta\cos\phi$
M_y	H_y	$\cos\phi$	$\cos\theta\sin\phi$
M_z	H_z	0	$\sin\theta$

angle diversities of these mutually orthogonal antenna patterns. To illustrate the inherent polarization and angle diversities in the six-element E/M dipole array, the radiation patterns of its elements are shown in Figures 2.1 and 2.2 for the ϕ- and θ-polarized fields, respectively. On the one hand, the orthogonality in the patterns can be seen from the viewpoint of angle diversity. The patterns of the array cover the whole sphere with each antenna element having its peak gain at distinct directions for a given polarization. On the other hand, the orthogonality can also be seen in terms of polarization diversity, where different antennas exhibit distinct polarization behaviors. The ϕ- and θ-polarized components of the patterns interchange between the electric and magnetic dipoles. For instance, the ϕ-polarized patterns of the electric dipoles in Figures 2.1(a), 2.1(c) and 2.1(e) become the θ-polarized patterns of the magnetic dipoles in Figures 2.2(b), 2.2(d) and 2.2(f). In other words, similar antenna patterns only occur for orthogonally polarized field components.

Throughout the analysis above, the co-located six-element E/M dipole array as sketched in Figure 1.10 is shown to offer good diversity characteristics. The correlation properties of the array are studied according to the discussion in Section 1.1.1, where the complex correlation coefficient between any two antenna elements $r_{k,l}$ of the correlation matrix $\mathbf{R}$ can be calculated using (1.10). In a uniform 3D propagation environment, the correlation matrix of $\mathbf{R} = \mathbf{I}_6$ (*i.e.*, 6×6 identity matrix) is obtained. In this case, full decorrelation is obtained, despite the six antennas being co-located. However, correlation can arise when the APS is of limited angular spreads. This is shown in Figure 2.3(a), where the maximum correlation, *i.e.*, the largest off-diagonal element of $\mathbf{R}$ is plotted with respect to different angular spreads in the Gaussian APS defined in (1.15). With larger angular spreads, the correlation becomes much smaller. However, the correlation increases with narrower angular spreads, which in turn leads to a reduced number of effective eigenchannels.

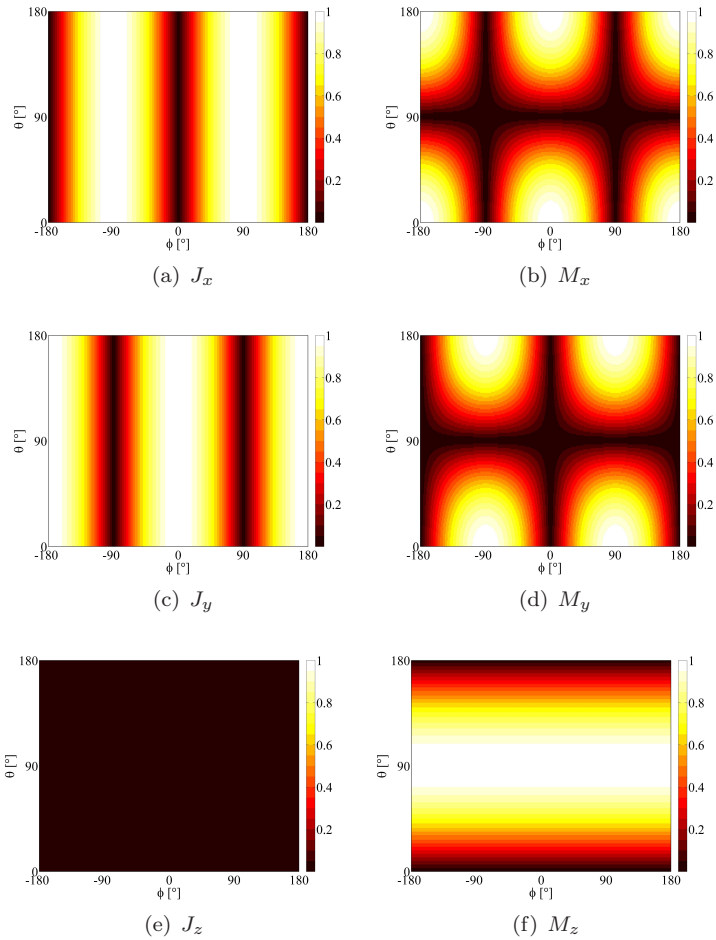

(a) J_x (b) M_x

(c) J_y (d) M_y

(e) J_z (f) M_z

Figure 2.1: $E_\phi(\theta, \phi)$ patterns of the six-element E/M dipole array in Figure 1.10.

The impact of angular spread on eigenchannels can be studied by investigating the eigenvalues of the MIMO channel matrix $\mathbf{H}$. Considering correlation at only one link end, the channel matrix can be obtained using the Kronecker channel model (1.24) with the correlation matrices $\mathbf{R}_{\mathrm{RX}} = \mathbf{R}$ and $\mathbf{R}_{\mathrm{TX}} = \mathbf{I}_6$. In Figure 2.3(b), the average eigenvalue flatness is illustrated for different angular spreads. As defined in (1.31), the flatness metric quantifies the dispersion

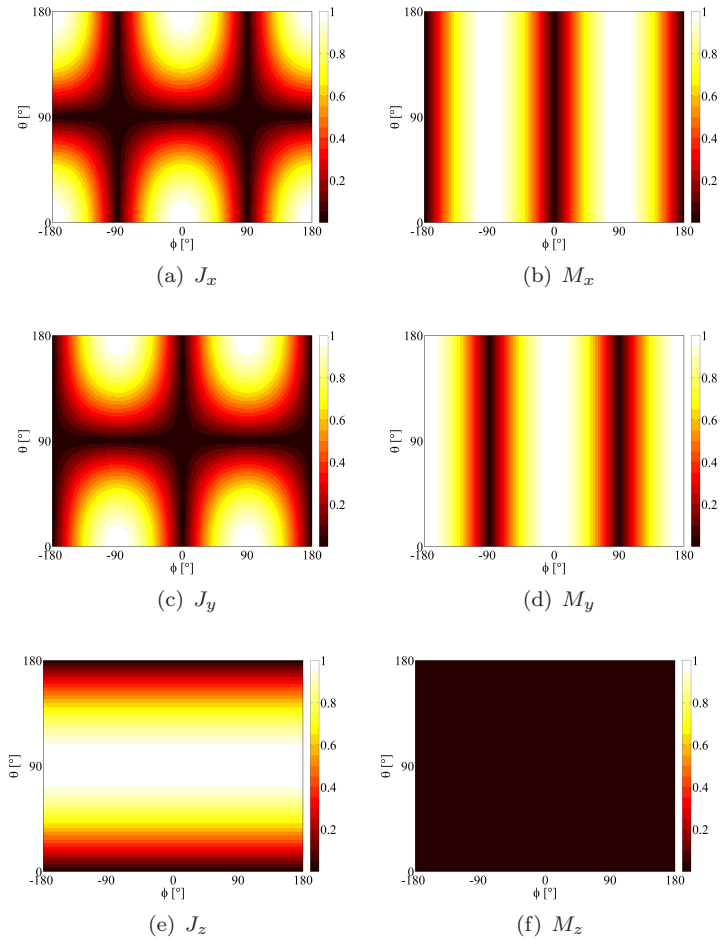

(a) J_x (b) M_x

(c) J_y (d) M_y

(e) J_z (f) M_z

Figure 2.2: $E_\theta(\theta, \phi)$ patterns of the six-element E/M dipole array in Figure 1.10.

of the eigenvalues, and a higher dispersion can be interpreted as a degradation in SNR [35]. Here, two types of six-element arrays are considered. In addition to the antenna array of co-located electric and magnetic dipoles, *i.e.*, the E/M dipole array as shown in Figure 1.10, a uniform linear array (ULA) of vertically polarized electric dipoles with inter-element separation of $d = \lambda_c/4$ is also studied for comparison. According to Figure 2.3(b), the dispersion of

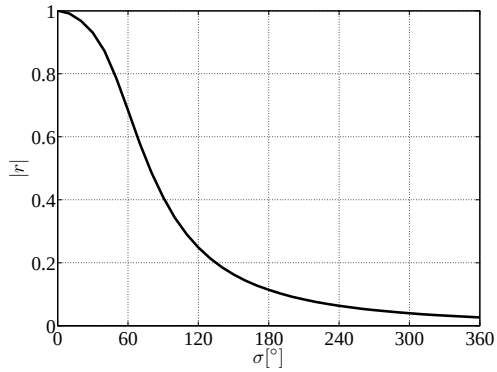

(a) Maximum cross-correlation

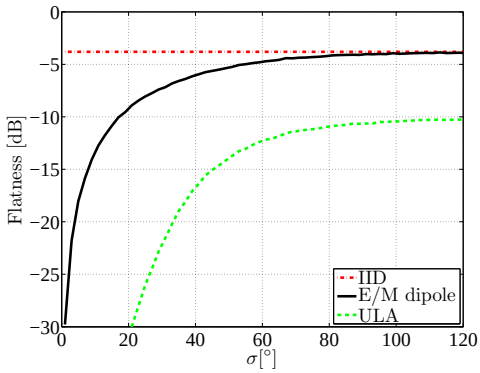

(b) Eigenvalue Flatness

Figure 2.3: Performance of the six-element array with the Gaussian APS centered at $(\theta_0 = 60°, \phi_0 = 0°)$ with angular spreads $\sigma_\theta = \sigma_\phi = \sigma$.

the eigenvalues is reduced with larger angular spreads, such that it is possible to exploit more eigenchannels. Using the E/M dipole array, the performance converges to that of the IID Rayleigh channel as the angular distribution approaches the uniform 3D case. Therefore, six eignechannels are only achievable using the E/M dipole array if the propagation channel is of rich multi-path scattering. However, the eigenvalue dispersion for the case of the ULA array is significant even with large angular spreads. This is because the ULA array with closely-spaced elements can only exploit space diversity to a limited extent.

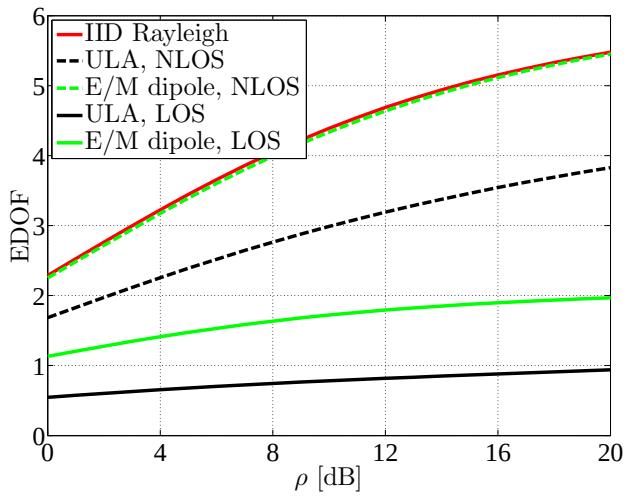

Figure 2.4: EDOF of the simulated channel.

To further study the behavior of the six-element E/M dipole array, the random scattering channel model discussed in Section 1.1.1 is used for simulation. The sketch of the simulated channel is given previously in Figure 1.5. In the simulation, 10^3 channel realizations are simulated, each of which consists of 10^2 randomly generated scatterers. In the NLOS scenario, the scatterers are uniformly generated with XPD $\chi = 1$. In the LOS scenario, however, the dominant scatterer is randomly assigned with the Rician K-factor of 20 dB. Similar to the study above, the same two six-element arrays are considered. In one case, the six-element E/M dipole array is used at both the TX and RX ends of the channel. In the other case, the ULA is employed at both ends.

The concept of EDOF has been defined in (1.32) to quantify the number of eigenchannels that can be efficiently utilized for spatial multiplexing. In Figure 2.4, the EDOF performance of the simulated channel using the two six-element arrays is shown. In the NLOS scenario, the E/M dipole array achieves similar performance as that of the IID Rayleigh channels. With high enough SNR, nearly six eigenchannels can be effectively exploited. However, this is not the case for the ULA which exploits space diversity to a limited extent. As a result, only four eigenchannels are obtained. On the other hand, with the dominant scatterer in the LOS scenario, only polarization diversity can be effectively exploited for providing the conventional two DOFs. This can be seen in Figure 2.4 that two eigenchannels are obtained using the E/M dipole

array. However, the ULA manages to attain merely one eigenchannel due to the use of single-polarized antennas.

Another approach to study this problem is to consider the MIMO cube concept proposed in [30]. The MIMO cube consists of 12 electric dipoles as its 12 edges. For a very compact cube with side length of $0.05\lambda_c$, six eigenchannels are obtained theoretically from simulations using a random scattering channel model. The result can be understood by considering that the four dipoles along each face of the cube can be thought of as a current loop. However, the first results are obtained by neglecting the mutual coupling effects among the antennas. If mutual coupling is considered in the simulation, the study in [68] shows that the six-eigenchannel results will no longer hold when the the side length of the cube is as small as $0.05\lambda_c$. In fact, the side length of the cube needs to be increased to about $0.2\lambda_c$ in order to obtain six DOFs using the 12-element MIMO cube. This observation sheds some light on the impact of mutual coupling in realizing physically compact arrays that can effectively offer six eigenchannels.

2.2 Experimental Implementation

Although it has been shown that the six-element E/M dipole array as sketched in Figure 1.10 can theoretically extract six DOFs from wireless channels with rich multi-path scattering, this interesting result has not been verified experimentally. The experiments performed in [40] manage to demonstrate only three DOFs by means of tri-polarized half-wave sleeve dipoles, rather than the postulated six-fold capacity increase. Moreover, the study of [42] also concludes that the use of half-wave dipoles and full-wave loops fails to attain six DOFs. This is because a current loop can only be considered as a magnetic dipole if the size of the loop is electrically small [12]. Otherwise, the orthogonality in the radiation patterns among the array elements cannot be maintained. However, electrically small antennas have fundamental limitations and they are difficult to implement [69, 70]. For instance, it is difficult to achieve good impedance matching to obtain reasonable antenna efficiency and operating bandwidth. Moreover, when multiple antennas are closely placed, mutual coupling effects need to be carefully accounted for. Otherwise, not only will the efficiencies of the antennas be impaired, but also the orthogonality in their patterns cannot be maintained. To the best of the author's knowledge, no six-element array as the one in Figure 1.10 has yet been implemented to successfully verify the availability of six DOFs in experiments. Instead, several attempts have been made in order to take advantage of this concept.

In [71,72], two DOFs are demonstrated by the use of co-located, co-polarized

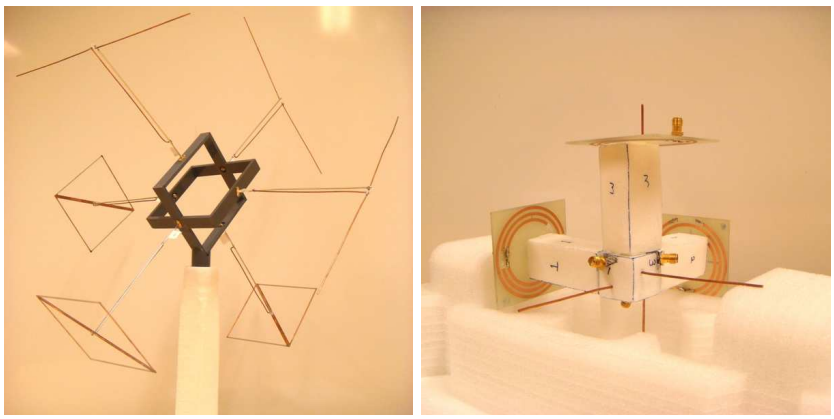

(a) TX Array (b) RX Array

Figure 2.5: Two six-element antenna arrays studied in [46].

electric and magnetic dipoles, where the magnetic dipole antenna is realized by a Kandoian loop [73] and an Alford loop [74], respectively. The design principle of these loop antennas is to maintain a uniform current distribution along the circumference of the loop while keeping the antenna at a reasonable size for good matching. Three-port arrays of orthogonally polarized dipoles or slots are designed in [75] and [76]. In [77], a four-port prototype is designed by combining tri-polarized dipoles with a loop antenna, where the loop is realized by means of four sectors that are fed in phase at their corners. This is also to maintain a uniform current distribution along the circumference of the loop in order to attain the desired characteristics of a magnetic dipole. While these experiments are performed successfully, however, they cannot conclusively show the possibility of extracting six DOFs from wireless channels with compact arrays of co-located elements. Therefore, the practical design and measurement of such an array remains an interesting challenge. In [78–80], conceptual six-element E/M dipole array prototypes similar to that of Figure 1.10 are proposed analytically and studied only by simulations. In addition, other multi-port arrays with more practical antennas have been also suggested. In [81], a six-port cube antenna of size $(0.43\lambda_c)^3$ is designed by combining tri-polarized patch and slot antennas. Furthermore, prototypes of the MIMO cube with 24 and 36 ports are designed in [82] using slot antennas.

One of the goals of this thesis is the experimental implementation of compact and co-located six-element MIMO arrays that can take full advantage of the DOFs in a wireless channel. In [46], two six-port antenna arrays are de-

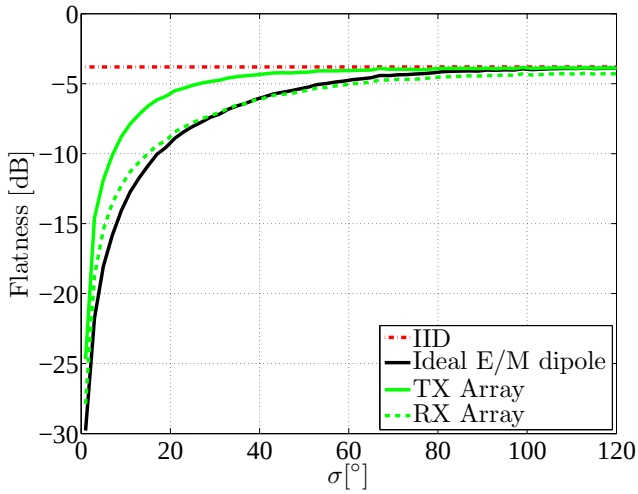

Figure 2.6: Eigenvalue flatness of the TX and RX arrays with the Gaussian APS centered at $(\theta_0 = 60°, \phi_0 = 0°)$ with angular spreads $\sigma_\theta = \sigma_\phi = \sigma$.

signed for this purpose. The fabricated prototypes are shown in Figure 2.5. The antenna elements of both prototypes are designed to yield the desired characteristics of fundamental electric and magnetic dipoles. In particular, one array (RX) is made compact with all antenna elements enclosed in a small spatial volume of $(0.24\lambda_c)^3$. The three electric dipoles are essentially co-located at the center of the array, whereas the magnetic dipoles are placed at about $0.1\lambda_c$ away from the array center. The achieved compactness is a substantial improvement in comparison to existing implemented designs in the literature. In fact, the achieved size approaches the analytical limit obtained from [68], where the 12-element MIMO cube needs to be about $(0.2\lambda_c)^3$ in order to obtain six DOFs, if the mutual coupling is taken into account.

The performance of the two fabricated six-port antenna arrays is compared to that of the ideal E/M dipole array. Using the measured radiation patterns of the antenna elements, the correlation matrices $\mathbf{R}_{\mathrm{TX}}$ and $\mathbf{R}_{\mathrm{RX}}$ of the TX and RX arrays are obtained using (1.10). In a uniform 3D APS scenario, the correlation coefficients of the TX and RX arrays are found to be lower than 0.13 and 0.32, respectively. To isolate the performance impact of the non-ideal TX and RX arrays over different angular spreads, we calculate the average eigenvalue flatness separately for these arrays. In particular, the channel for

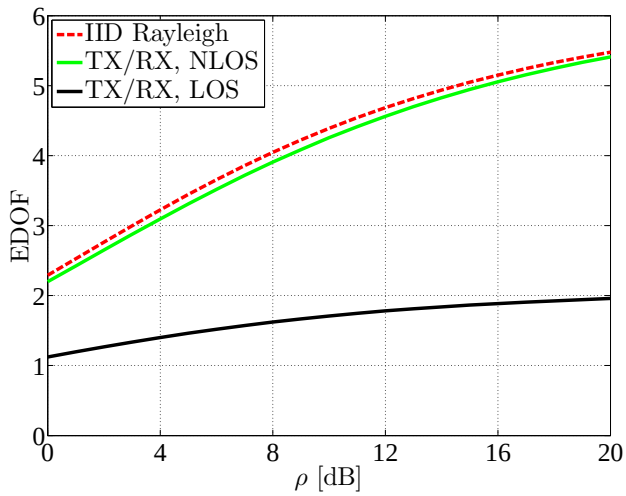

Figure 2.7: EDOF of the simulated channel using the random scattering model with the TX/RX arrays.

the TX array assumes the receive correlation $\mathbf{R}_{\mathrm{RX}} = \mathbf{I}_6$, whereas the channel for the RX array assumes $\mathbf{R}_{\mathrm{TX}} = \mathbf{I}_6$. For the case of the Gaussian APS scenario, the average eigenvalue flatness obtained from the channel matrix is illustrated in Figure 2.6. According to the result, the performance of both arrays converges to that of the IID Rayleigh channel for large enough angular spreads. It is noted that the TX array achieves better performance than the ideal E/M dipole array for the case of narrow angular spreads. This is because of the TX array's significantly larger size, *i.e.*, it is confined within a cube of $(0.75\lambda_{\mathrm{c}})^3$. In that case, space diversity is exploited to a certain extent, which contributes to improve the performance as angle diversity becomes less effective with narrowly distributed APS. However, this is not the case for the compact RX array, which shares a similar performance as that of the ideal E/M dipole array. This result indicates that space diversity is limited in the RX array, such that the achieved performance is mainly attributed to polarization and angle diversities.

The two arrays are further investigated using the random scattering model in Figure 1.5. The EDOF performance of the simulated channel using the TX/RX arrays is shown in Figure 2.7. The figure shows that the use of the two arrays achieves similar performance as that of the IID Rayleigh channels in the NLOS scenario. With high enough SNR, six eigenchannels can be effectively

exploited for spatial multiplexing. On the other hand, only two DOFs can be utilized in the LOS scenario. Details of the antenna design and its experimental evaluation can be found in the included Paper I of the thesis.

Further, in order to study the potential of implementing different diversity mechanisms on a practical multi-port antenna, a compact six-port dielectric resonator antenna (DRA) array is investigated in [47]. The DRA is based on a suitably shaped dielectric material, which has been shown by many early studies [83–85] as electrical resonators for high frequency oscillations. More recently, their application as antenna elements has also been demonstrated [86–88]. One interesting feature of the DRA is that the antenna can be electrically small when dielectric material with high permittivity is used. This makes it attractive for compact implementations in wireless communication applications. The six-port DRA array proposed in [47] is based on an existing rectangular DRA element [89] which supports two fundamental transverse electric (TE) modes that radiate like magnetic dipoles. A monopole antenna is inserted into the center of the element to introduce a third mode without disturbing the radiating modes of the dielectric resonator. Two such compact DRA elements of size $0.16\lambda_c \times 0.16\lambda_c \times 0.12\lambda_c$ are placed on a large ground plane with a separation distance of $0.44\lambda_c$. The six-port array simultaneously utilizes space, polarization and angle diversities such that it exploits all available DOFs. Good spatial multiplexing performance is achieved with the DRA array in an office environment at 2.65 GHz, which mimics a typical wireless LAN scenario. The array design and evaluation are discussed in details as Paper II.

Chapter 3

Multi-antenna System Characterization

Designing antennas for mobile terminal devices is a challenging task. Along with the worldwide evolution of wireless systems, the required number of frequency bands at which the antennas should be operating has been constantly increasing. However, the space dedicated for the multi-band antennas has been limited due to the compactness of the chassis. Moreover, the problem of near-field disturbances from the user can severely degrade link quality, as has been the case recently for one of the most popular mobile terminal devices.

Recently, MIMO technology has been adopted in all major wireless standards. This requirement of multiple co-band antennas further complicates the antenna design problem. In particular, if we consider the LTE system operating at 700 MHz, the required separation distance of $\lambda_c/4$ for achieving reasonably low correlation of 0.7 is about 10 cm. This distance is around the size of the latest smart phones with 4.3 inch touch screens. Moreover, significant mutual coupling also arises in closely spaced multi-antenna systems. As discussed in Section 1.2.2, mutual coupling can lead to not only high correlation but also severe loss in efficiency of the antenna system. In addition, it has been found that the characteristic modes of the antenna chassis also need to be accounted for in order to obtain the optimal radiation performance of the antennas [90].

Whereas antennas have been known to play a major role in determining the performance of a wireless system, it is the propagation channel that imposes the fundamental limitation on MIMO performance (given the optimal antenna system for the channel). Therefore, the interaction between the antennas and the channel should be appropriately characterized. These considerations render

the design of multi-antenna systems a very challenging task.

3.1 Single-antenna Performance

Conventionally, antennas are mainly characterized by their frequency bandwidth and radiation performance. The operating bandwidth is defined from the reflection coefficient of the antenna as measured using a vector network analyzer (VNA). The radiation performance of the antenna is characterized by either a passive or an active measurement performed in a radio anechoic chamber. In the passive measurement, the antenna is connected directly to the feed cable and its far-field radiation pattern is obtained. The measured pattern is then used to determine the radiation efficiency, directivity and gain of the antenna. The active measurement characterizes the over-the-air (OTA) performance of the antenna using power based metrics such as total radiated power (TRP) and total isotropic sensitivity (TIS), which are measured in decibel. Active measurements are performed with the device activated and without external cable connections, which ensure that the actual performance of the device is obtained. It is worth noting that TRP and TIS can also be obtained with a reverberation chamber [91]. Typically, the desired characteristics of single-antenna systems include multiple frequency bands coverage, high efficiency and omni-directional radiation pattern.

The impact of the environment surrounding the antenna system is further considered in more advanced methods for antenna characterization. The user of the device is known to introduce near-field interferences, which can have a significant impact on the antenna performance [33, 92, 93]. The interaction of an antenna with a propagation channel can be characterized using the concept of MEG (1.11) as discussed in Section 1.1.1. In addition, the double-directional concept of the physical channel models provides a way for separate modeling of the antenna system and the channel [27]. Using this approach, the propagation characteristics can be modeled based on measurements performed using a channel sounder and a calibrated multi-antenna system. The radiation characteristics of the antennas can be combined with the double-directional channel models in post-processing, allowing a realistic evaluation of the antenna performance. This approach can be further extended by considering the user as an integral part of the antenna, forming a super-antenna concept [93]. For further verifications, the antenna system can be evaluated directly in its actual usage conditions through field tests using a network analyzer or a channel sounder.

3.2 Multi-antenna Performance

When it comes to performance characterization of multi-antenna systems, the single-antenna metrics and approaches remain meaningful and important. However, more issues should be addressed. For example, as discussed previously, correlation between antenna elements has a strong impact on the performance of different space-time processing techniques. Given the radiation patterns of the antennas and the statistical distribution of the propagation channel, the correlation can be evaluated using (1.10). Following that, channel matrix can be composed using one of the analytical models for further evaluation. Channel matrices can also be composed using physical channel models together with the radiation patterns of the multi-element antennas.

The above way of characterizing multi-antenna systems relies on accurate measurements of radiation patterns for all antenna elements. However, a sophisticated measurement system is required in order to obtain both magnitude and phase patterns. Moreover, the phase information is usually not available in active measurements of mobile terminals. The effects of using phaseless patterns are evaluated in [94, 95], showing that unacceptable underestimation of MIMO performance is obtained. Simple and improved approaches have been proposed in [95] to reduce the performance estimation errors.

Another challenge in characterizing multi-antenna performance is that many parameters are important in determining the overall performance, and these include efficiency, correlation, power imbalance, etc. In the course of this thesis work, it has been found that existing performance metrics do not adequately isolate the impact of different antenna impairments on the performance of MIMO systems or give a definitive measure of performance difference between efficient and less efficient multi-antennas. When diversity techniques are applied to mitigate multi-path fading, the performance gain is typically expressed as diversity gain in terms of power advantage. Such a measure is convenient for antenna design, since the improvement is translated into a tangible power gain, or equivalently, an increase in coverage area. On the other hand, when spatial multiplexing schemes are applied, the information theoretic capacity has been the performance measure of choice. Different multi-antenna systems are usually evaluated and compared by their differences in terms of channel capacity. However, capacity is a system level metric that is less intuitive to antenna designers, who would benefit more from a power related measure, such as the diversity gain.

In response, multiplexing efficiency is proposed in [96] as a performance metric for the design and evaluation of multi-antenna systems. Multiplexing efficiency η_{mux} measures the loss of efficiency in power when using a real multi-antenna prototype to achieve the same multiplexing performance as that of an

ideal array in the same propagation channel. For the case of a two-element MIMO system with a uniform 3D channel, η_{mux} is given by a simple and intuitive expression as

$$\eta_{\text{mux}} = \sqrt{\eta_1 \eta_2 (1 - |r|^2)}, \tag{3.1}$$

where η_1 and η_2 are the total efficiencies of antennas 1 and 2, respectively. The expression consists of a term of $\sqrt{\eta_1 \eta_2}$, which is the geometric mean of the total efficiencies of the two antennas. This term quantifies the average efficiency of the antennas (in dB), as well as the efficiency imbalance, since the geometric mean describes the flatness of the branch power. The remain term describes the loss of efficiency as induced by the antenna correlation r. The usage of this metric can be generalized to random propagation environments in a straightforward manner, as the MEG and the correlation can be evaluated for a channel with an arbitrary APS according to what has been discussed in Section 1.1.1.

The multiplexing efficiency metric is derived in detail in Paper IV of this thesis. The numerical study on practical multi-antenna prototypes highlights the effectiveness of the metric in identifying and addressing critical design parameters of multi-antenna systems.

Chapter 4

Contributions and Conclusions

In this chapter, the contributions of this thesis to the research field are summarized. Section 4.1 provides a summary for each of the five included research papers. It also specifies my contributions to each of the papers. Some general conclusions and suggestions on future work are discussed in Section 4.2.

4.1 Research Contributions

4.1.1 Paper I: "Experimental Verification of Degrees of Freedom for Co-located Antennas in Wireless Channels"

One of the challenges in designing multi-antenna systems is to efficiently exploit as many eigenchannels as are available in the propagation channel. Conventional systems with spatially separated antenna elements perform best when spatial correlations among signals on different antenna branches are low. This typically requires the antenna elements to be separated by one half of a wavelength ($0.5\lambda_c$), which is not always feasible in some applications. On the other hand, the use of the two polarization states of plane waves has been known to introduce two DOFs. This so called polarization diversity has the benefit that low correlation can be achieved using co-located antennas. Furthermore, in a rich multi-path scattering environment, it has been claimed that six distinguishable electric and magnetic field components are able to introduce six DOFs. It is further postulated that six co-located orthogonally polarized electric and

magnetic dipoles can offer six DOFs and hence a six-fold capacity increase in the context of MIMO systems, relative to conventional SISO systems. However, due to the complexity of designing and measuring such a six-port antenna array, there has been no successful experimental verification of this theoretical hypothesis.

In this paper, the six DOFs hypothesis is experimentally verified at 300 MHz. The experiment involves the design and fabrication of two six-port arrays. The antenna elements of both prototypes are designed to yield the desired characteristics of fundamental electric and magnetic dipoles. In particular, one array is made compact with all antenna elements enclosed within a small spatial volume of $(0.24\lambda_c)^3$. The three electric dipoles are co-located at the center of the array, whereas the magnetic dipoles are placed at about $0.1\lambda_c$ away from the array center. The implemented array is significantly smaller than existing compact six-port array designs in the literature. Using the two arrays, MIMO channel measurements are performed in a RF shielded laboratory in order to obtain a rich multi-path scattering environment. Analysis on measured channel eigenvalues shows that six eigenchannels are attained, and they closely resemble those offered by the IID Rayleigh channels, with only a small degradation. Using the Kronecker model, the investigation also reveals that the small performance degradation obtained from the measurements can be mainly attributed to practical constraints in achieving perfect six-port antenna arrays.

I am the main contributor to this paper. I have been involved in all parts of the scientific work, including antenna design, fabrication and characterization, channel measurement and its planning, data analysis and manuscript writing.

4.1.2 Paper II: "A Compact Six-port Dielectric Resonator Antenna Array: MIMO Channel Measurements and Performance Analysis"

To further study the potential of implementing different diversity mechanisms on a practical compact multi-port antenna, this paper develops another six-port antenna array. The proposed array consists of two three-port DRA elements, which jointly utilizes space, polarization and angle diversities. One interesting feature of the DRA is that the antenna can be made very compact when dielectric material with high permittivity is used. This makes the DRA an attractive solution for compact implementations in wireless devices. Two compact DRA elements of size $0.16\lambda_c \times 0.16\lambda_c \times 0.12\lambda_c$ are placed on a ground plane with a separation distance of $0.44\lambda_c$.

In order to fully substantiate the practicality of the DRA array in its usage environment, a measurement campaign was conducted at 2.65 GHz in indoor

office scenarios with four different 6×6 multi-antenna systems. In addition to the compact DRA array, two common types of six-port antenna arrays were also measured for the purpose of comparison: a single-polarized monopole array that exploits only space diversity, and a dual-polarized patch array that exploits both space and polarization diversities.

Several performance metrics are evaluated, including power efficiency, branch imbalance and channel capacity. When compared to the reference system of monopole arrays which only exploits space diversity, the use of dual-polarized patch antennas at the transmitter enriches the DOF of the channel in the NLOS scenario. Replacing the monopole array at the receiver with the DRA array that has a 95% smaller ground plane, the 10% outage capacity evaluated at 10 dB SNR is the same as that of the reference system. The effective miniaturization of the array is possible due to the DRA's rich diversity characteristics. In the LOS scenario, the DRA array gives a higher DOF than the monopole array as the receive counterpart to the transmit patch array. However, the outage capacity is 1.5 bps/Hz lower, due to the lower antenna gain of the DRA array.

This work has been carried out in cooperation with Sony Ericsson and the evaluated compact DRA array is derived from their patent application on the single DRA element. The paper focuses on the performance evaluation of the DRA array in real office environments. I am the main contributor to this paper. I have been involved in all parts of the scientific work, including channel measurement and its planning, data analysis and manuscript writing.

4.1.3 Paper III: "Uncoupled Antenna Matching for Performance Optimization in Compact MIMO Systems using Unbalanced Load Impedance"

Some applications of multi-antenna systems require antenna elements to be closely spaced. This leads to high electromagnetic interactions among the antenna elements, known as mutual coupling. Mutual coupling is a key concern for MIMO systems since strong coupling can lead to not only high correlation but also severe loss of efficiency in the antenna system.

To counteract the effects of mutual coupling, recent work has shown that impedance matching networks can be utilized. For example, the optimal performance can be achieved if a sophisticated multi-port matching network is utilized. Interestingly, the optimal multi-port network is simply an extension of the single-antenna conjugate match to the multi-port case. However, such a coupled matching network is difficult to construct, and can be quite lossy in general. As a result, a simple uncoupled (or individual port) impedance matching network is adopted in this paper. It has been shown that the un-

coupled matching networks could be optimized against a given performance metric with the constraint of having the same matching (or equivalent load) impedance value for all antennas, *i.e.*, balanced matching.

In this paper, we extend the study of uncoupled matching in several ways. First, we increase the DOFs in the uncoupled matching network by introducing unbalanced networks, where different antenna ports may be terminated by arbitrary matching impedances. Second, we investigate the performance optimization in terms of received power as well as mean capacity with both balanced and unbalanced matching impedances, under the scenarios of uniform and Laplacian APS. Moreover, we study the effects of having different array sizes and topologies.

Numerical studies suggest that the achieved improvement with unbalanced matching varies with the array topology and the propagation environment, when compared to balanced matching. For example, we can improve the total mean received power by up to 1.6 dB and the channel capacity by up to 23% when matching a three-dipole ULA to propagation environments that are asymmetrical about the array broadside, whereas the symmetrical environments do not benefit as much from unbalanced matching. We conclude that unbalanced matching is especially effective for arrays with effective apertures that can vary significantly with respect to the propagation environment. Moreover, it is also demonstrated that the unbalanced matching is capable of adapting (or beamforming) the radiation patterns of the array elements to the dynamic directional propagation environment.

I am the main contributor to this paper. I have been involved in all parts of the scientific work, including model derivation and simulation, numerical analysis and manuscript writing.

4.1.4 Paper IV: "Multiplexing Efficiency of MIMO Antennas"

With the recent adoption of MIMO technology in major wireless communication standards, performance characterization of multi-antenna systems on wireless terminals is a subject of current interest. However, it has been found that existing performance metrics do not adequately isolate the impact of different antenna impairments on the performance of MIMO systems or give a definitive measure of performance difference between efficient and less efficient multi-antennas. In response, we propose a simple and intuitive metric that fully meets these requirements.

This paper introduces multiplexing efficiency as a power related metric for characterizing the multiplexing capability of MIMO antennas. It is defined as the loss of efficiency in decibel when using a multi-antenna prototype under test

to achieve the same capacity as that of an ideal array in the same propagation channel. A closed form expression is derived for the case of a channel with uniform 3D APS. The unique features of the expression are both its simplicity and the valuable insights it offers with respect to the performance impact of non-ideal behaviors on the multi-antenna systems. As an example, the metric is applied to demonstrate its effectiveness in distinguishing between two realistic mobile terminal prototypes. One prototype is found to be 3 dB more efficient in multiplexing efficiency than the other. Numerically, the higher average antenna efficiency contributes to a gain of 1 dB in the better terminal, whereas the high correlation of 0.8 in the worse terminal causes a further 2 dB loss in multiplexing efficiency with respect to the better terminal that has a low correlation of 0.2

This work has been carried out in cooperation with Sony Ericsson using their antenna prototypes. I am the main contributor to this paper. I have been involved in all parts of the scientific work, including model derivation and simulation, numerical analysis, experimental evaluation and manuscript writing.

4.1.5 Paper V: "On MIMO Performance Enhancement with Multi-sector Cooperation in a Measured Urban Environment"

This paper extends the discussion of multi-antenna systems to their usage in cellular systems. In order to further improve the average system throughput particularly in cell edge regions, more advanced MIMO techniques involving cooperation among antennas at different geographical locations are being considered.

In this paper, the single-user capacity improvement of intrasite multi-sector cooperation involving three 120°-sectors of a single BS site is investigated in a measured urban macrocellular environment. The results show that the mean capacity gain exceeds 40% in as much as 1/4 of the coverage area, relative to single-sector links with no cooperation. The improvement is most significant at the sector edges, where it is most needed. In addition, to analyze the impact of BS antennas and specific propagation mechanisms on the measured cooperative gain, a simple simulation model is developed based on a "one-ring" channel model and measured antenna patterns. The model exhibits good accuracy, as the simulated cooperative gain is mostly within one standard deviation of the measured gain. The discrepancies between the simulated and measured cooperative gains can be attributed to propagation mechanisms that are not accounted for in the model.

This work was carried out in cooperation with Ericsson Research in Kista using their measurement data. I am the main contributor to this paper. I have

been involved in all parts of the scientific work, including derivation of theoretical model and simulation, measurement analysis and manuscript writing.

4.2 Conclusions and Outlook

The overarching question that this thesis tries to answer is: how to design compact yet efficient multi-antennas to deliver a MIMO system with high performance? This thesis provides an overview of the state of the art, and extends the understanding of MIMO systems from an antenna and propagation perspective.

Designing compact yet efficient MIMO antennas is a very challenging task. Although antennas are known to be a vital part of the overall radio system, they are usually simplified in system-related studies. As a result, at least on the user terminal side of a SISO system, an antenna with high efficiency and omni-direction radiation is considered good enough. In fact, both of the two above merits are still highly desirable when it comes to designing MIMO antennas. High efficiency is important since the power loss due to antennas with low efficiencies cannot be compensated even with advanced baseband signal processing techniques. The omni-direction radiation pattern is also favored by the dynamic environment in which the user will experience in reality.

However, these guidelines are not sufficient for designing efficient MIMO antennas. For instance, in the case of spatial multiplexing schemes, space-time processing facilitates parallel transmission of data streams. Correspondingly, efficient MIMO antennas should be able to offer the system the capability for accessing these orthogonal eigenchannels. One basic requirement is that the correlation among the different TX-RX channels should be kept reasonably low. The propagation channel is determined by the local scattering environment, whereas the antennas will determine how the channel is sampled from the viewpoint of the system. Given a large angular spread of the incident field, co-polarized multi-antennas that have omni-direction radiation patterns will still require significant spatial separation to exploit space diversity and reduce correlation. If the antennas need to be closely spaced due to the constraint imposed by the application in question, it becomes an inefficient MIMO antenna. Furthermore, mutual coupling also becomes significant and needs to be properly addressed in such a design. However, if the pattern of each antenna element is designed to cover a distinct angular region, they can be placed closer, and at the same time achieve orthogonal eigenchannels by means of angle diversity. On the other hand, angle diversity becomes less effective if the scattering environment has narrow angular spreads. Some eigenchannels cannot be exploited because not all antennas are matched to the propagation channel. The

remedy for this case is to exploit polarization diversity.

The major part of the thesis is dedicated to offer valuable insights on the design of compact multi-antennas for efficient MIMO communications. In the course of the thesis work, several multi-port antennas have been designed, fabricated and evaluated. The fundamental question on the number of DOFs that can be efficiently exploited in a multi-path propagation channel is explored with a comprehensive measurement campaign. As a result, six eigenchannels are attained using co-located antenna arrays of orthogonally polarized electric and magnetic dipoles. This array has achieved by far the most compact six-port antenna structure which offers a performance closely resembling that of the theoretical limit. Another more practical MIMO antenna is also designed as a compact six-port DRA array. The evaluation of the six-port DRA array in realistic usage scenario shows that the compact array can offer equivalent MIMO performance as that of a much larger array due to its simultaneous utilization of space, angle and polarization diversities.

To further support the development of MIMO antennas for compact device applications, the thesis also examines the potential of adaptively optimizing the impedance matching network of the antenna system to its dynamic usage environments. The study illustrates that the approach is especially effective for array topology whose effective aperture can vary significantly with respect to the propagation channel. Furthermore, a simple and intuitive metric is proposed which clearly isolates the impact of different antenna impairments and gives a definitive measure of the performance difference between efficient and less efficient MIMO antennas. Finally, cooperation among multi-sector BS MIMO antennas is investigated in a cellular system. Significant performance benefit is achieved at sector edges, where the improvement is most needed.

For future work, the method proposed in [58] is of great interest, since it provides a framework for determining the optimal antenna radiation characteristics, given the propagation channel, *i.e.*, optimal sampling of the incident field. It will be interesting to study if this method can also be taken into account in exploiting available DOFs. A possible approach to achieve this is to apply the importance sampling method for statistical modeling of the antenna and the propagation channel. Another future aspect is to investigate cooperative MIMO with distributed antenna systems, *e.g.*, in sensor networks. The research in Paper V can be extended by considering cooperation of antennas located at different BS and MS locations, formulating a distributed-input and distributed-output system. Time variance, interference modeling and resource allocation are of interest in this problem. Last but not least, it would be interesting to apply more aspects of electromagnetic theory in MIMO research, since both these topics exploit the physics of space and time.

References

[1] C. E. Shannon, "A mathematical theory of communication," *Bell System Technical Journal*, vol. 27, pp. 379 – 423, 623 – 656, July and October 1948.

[2] E. Dahlman, S. Parkvall, J. Sköld, and P. Beming, *3G Evolution: HSPA and LTE for Mobile Broadband, 2nd Edition*. Academic Press, 2008.

[3] B. Mishkind, "The Marconi archive section of the broadcast archive." `http://www.oldradio.com/archives/jurassic/marconi.htm`.

[4] A. Paulraj, D. Gore, R. Nabar, and H. Bölcskei, "An overview of MIMO communications - a key to gigabit wireless," *Proceedings of the IEEE*, vol. 92, pp. 198 – 218, Feb. 2004.

[5] J. Winters, "On the capacity of radio communication systems with diversity in a Rayleigh fading environment," *IEEE Journal on Selected Areas in Communications*, vol. 5, pp. 871 – 878, June 1987.

[6] G. J. Foschini and M. J. Gans, "On limits of wireless communications in a fading environment when using multiple antennas," *Wireless Personal Communication*, vol. 6, pp. 311 – 335, 1998.

[7] I. E. Telatar, "Capacity of multi-antenna Gaussian channels," *European Transactions on Telecommunications*, vol. 10, pp. 585 – 595, 1999.

[8] A. F. Molisch, *Wireless Communications*. Wiley-IEEE Press, 2005.

[9] J. Proakis, *Digital Communications, 4th Edition*. McGraw-Hill, 2001.

[10] R. Vaughan and J. B. Andersen, *Channels, Propagation and Antennas for Mobile Communications*. London: The IEE, 2003.

[11] T. Taga, "Analysis for mean effective gain of mobile antennas in land mobile radio environments," *IEEE Transactions on Vehicular Technology*, vol. 39, pp. 117 – 131, May 1990.

[12] C. A. Balanis, *Antenna Theory: Analysis and Design, 3rd Edition*. Wiley-Interscience, 2005.

[13] J. Fuhl, A. Molisch, and E. Bonek, "Unified channel model for mobile radio systems with smart antennas," *IEE Proceedings on Radar, Sonar and Navigation*, vol. 145, pp. 32 – 41, Feb. 1998.

[14] W. Lee and Y. Yeh, "Polarization diversity system for mobile radio," *IEEE Transactions on Communications*, vol. 20, pp. 912 – 923, Oct. 1972.

[15] R. Vaughan, "Polarization diversity in mobile communications," *IEEE Transactions on Vehicular Technology*, vol. 39, pp. 177 – 186, Aug. 1990.

[16] R. Nabar, H. Bolcskei, V. Erceg, D. Gesbert, and A. Paulraj, "Performance of multiantenna signaling techniques in the presence of polarization diversity," *IEEE Transactions on Signal Processing*, vol. 50, pp. 2553 – 2562, Oct. 2002.

[17] V. Erceg, P. Soma, D. Baum, and S. Catreux, "Multiple-input multiple-output fixed wireless radio channel measurements and modeling using dual-polarized antennas at 2.5 GHz," *IEEE Transactions on Wireless Communications*, vol. 3, pp. 2288 – 2298, Nov. 2004.

[18] H. Asplund, J.-E. Berg, F. Harrysson, J. Medbo, and M. Riback, "Propagation characteristics of polarized radio waves in cellular communications," in *IEEE 67th Vehicular Technology Conference (VTC)*, pp. 839 – 843, Baltimore, MD, USA, Oct. 2007.

[19] C. Oestges, B. Clerckx, M. Guillaud, and M. Debbah, "Dual-polarized wireless communications: from propagation models to system performance evaluation," *IEEE Transactions on Wireless Communications*, vol. 7, pp. 4019 – 4031, Oct. 2008.

[20] M. Coldrey, "Modeling and capacity of polarized MIMO channels," in *IEEE 67th Vehicular Technology Conference (VTC)*, pp. 440 – 444, Singapore, May 2008.

[21] F. Quitin, C. Oestges, F. Horlin, and P. De Doncker, "Polarization measurements and modeling in indoor NLOS environments," *IEEE Transactions on Wireless Communications*, vol. 9, pp. 21 – 25, Jan. 2010.

[22] P. Almers, E. Bonek, A. Burr, N. Czink, M. Debbah, V. Degli-esposti, H. Hofstetter, P. Kyösti, D. Laurenson, G. Matz, A. F. Molisch, C. Oestges, and H. Özcelik, "Survey of channel and radio propagation models for wireless MIMO systems," *EURASIP Journal on Wireless Communications and Networking*, 2007.

[23] M. Jensen and J. Wallace, "A review of antennas and propagation for MIMO wireless communications," *IEEE Transactions on Antennas and Propagation*, vol. 52, pp. 2810 – 2824, Nov. 2004.

[24] A. Paulraj, R. Nabar, and D. Gore, *Introduction to Space-Time Wireless Communications*. New York: Cambridge University Press, 2003.

[25] J. Kermoal, L. Schumacher, K. Pedersen, P. Mogensen, and F. Frederiksen, "A stochastic MIMO radio channel model with experimental validation," *IEEE Journal on Selected Areas in Communications*, vol. 20, pp. 1211 – 1226, Aug. 2002.

[26] H. Özcelik, M. Herdin, W. Weichselberger, J. Wallace, and E. Bonek, "Deficiencies of Kronecker MIMO radio channel model," *Electronics Letters*, vol. 39, pp. 1209 – 1210, Aug. 2003.

[27] M. Steinbauer, A. F. Molisch, and E. Bonek, "The double-directional radio channel," *IEEE Antennas and Propagation Magazine*, vol. 43, no. 4, pp. 51 – 63, 2001.

[28] M. Gustafsson and S. Nordebo, "Characterization of MIMO antennas using spherical vector waves," *IEEE Transactions on Antennas and Propagation*, vol. 54, pp. 2679 – 2682, Sep. 2006.

[29] A. A. Glazunov, M. Gustafsson, A. Molisch, F. Tufvesson, and G. Kristensson, "Spherical vector wave expansion of Gaussian electromagnetic fields for antenna-channel interaction analysis," *IEEE Transactions on Antennas and Propagation*, vol. 57, no. 7, pp. 2055–2067, 2009.

[30] B. Getu and J. Andersen, "The MIMO cube - a compact MIMO antenna," *IEEE Transactions on Wireless Communications*, vol. 4, pp. 1136 – 1141, May. 2005.

[31] P. Almers, F. Tufvesson, and A. Molisch, "Keyhole effect in MIMO wireless channels: measurements and theory," *IEEE Transactions on Wireless Communications*, vol. 5, pp. 3596 – 3604, Dec. 2006.

[32] D. Tse and P. Viswanath, *Fundamentals of Wireless Communication*. Cambridge University Press, 2005.

[33] V. Plicanic, B. K. Lau, A. Derneryd, and Z. Ying, "Actual diversity performance of a multiband diversity antenna with hand and head effects," *IEEE Transactions on Antennas and Propagation*, vol. 57, no. 5, pp. 1547 – 1556, 2009.

[34] G. J. Foschini, "Layered space-time architecture for wireless communication in a fading environment when using multi-element antennas"," *Bell Laboratories Technical Journal*, pp. 41 – 59, Autumn 1996.

[35] P. Suvikunnas, J. Salo, L. Vuokko, J. Kivinen, K. Sulonen, and P. Vainikainen, "Comparison of MIMO antenna configurations: Methods and experimental results," *IEEE Transactions on Vehicular Technology*, vol. 57, pp. 1021 – 1031, Mar. 2008.

[36] H. Özcelik and C. Oestges, "Some remarkable properties of diagonally correlated MIMO channels," *IEEE Transactions on Vehicular Technology*, vol. 54, pp. 2143 – 2145, Nov. 2005.

[37] A. M. Tulino and S. Verdu, "Random matrix theory and wireless communications," in *Foundations and Trends in Communications and Information Theory*, Jun. 2004.

[38] D.-S. Shiu, G. Foschini, M. Gans, and J. Kahn, "Fading correlation and its effect on the capacity of multielement antenna systems," *IEEE Transactions on Communications*, vol. 48, pp. 502 – 513, Mar. 2000.

[39] J. D. Jackson, *Classical Electrodynamics, 3rd Edition.* New York: John Wiley, 1999.

[40] R. A. Andrews, P. P. Mitra, and R. deCarvalho, "Tripling the capacity of wireless communications using electromagnetic polarization," *Nature*, vol. 409, pp. 316 – 318, Jan. 2001.

[41] S. H. Simon, A. L. Moustakas, M. Stoytchev, and H. Safar, "Communication in a disordered world," *Physics Today*, vol. 54, no. 9, pp. 38 – 43, 2001.

[42] T. Svantesson, M. Jensen, and J. Wallace, "Analysis of electromagnetic field polarizations in multiantenna systems," *IEEE Transactions on Wireless Communications*, vol. 3, pp. 641 – 646, Mar. 2004.

[43] M. Migliore, "On the role of the number of degrees of freedom of the field in MIMO channels," *IEEE Transactions on Antennas and Propagation*, vol. 54, pp. 620 – 628, Feb. 2006.

[44] A. Poon, R. Brodersen, and D. Tse, "Degrees of freedom in multiple-antenna channels: a signal space approach," *IEEE Transactions on Information Theory*, vol. 51, pp. 523 – 536, Feb. 2005.

[45] M. S. Elnaggar, S. K. Chaudhuri, and S. Safavi-Naeini, "Multi-polarization dimensionality of multi-antenna systems," *Progress In Electromagnetics Research B*, vol. 14, no. 2, pp. 45 – 63, 2009.

[46] R. Tian and B. K. Lau, "Experimental verification of degrees of freedom for co-located antennas in wireless channels," *IEEE Transactions on Antennas and Propagation*, 2011 (Submitted).

[47] R. Tian, V. Plicanic, B. K. Lau, and Z. Ying, "A compact six-port dielectric resonator antenna array: MIMO channel measurements and performance analysis," *IEEE Transactions on Antennas and Propagation*, vol. 58, pp. 1369 – 1379, Apr. 2010.

[48] B. K. Lau, "Multiple antenna terminals," in *MIMO: From Theory to Implementation*, C. Oestges, A. Sibille, and A. Zanella Eds. San Diego: Academic Press 2011.

[49] P. S. Kildal and K. Rosengren, "Electromagnetic analysis of effective and apparent diversity gain of two parallel dipoles," *IEEE Antennas and Wireless Propagation Letters*, vol. 2, no. 1, pp. 9 – 13, 2003.

[50] J. Wallace and M. Jensen, "Termination-dependent diversity performance of coupled antennas: network theory analysis," *IEEE Transactions on Antennas and Propagation*, vol. 52, pp. 98–105, Jan. 2004.

[51] J. Wallace and M. Jensen, "Mutual coupling in MIMO wireless systems: a rigorous network theory analysis," *IEEE Transactions on Wireless Communications*, vol. 3, pp. 1317 – 1325, Jul. 2004.

[52] B. K. Lau, J. B. Andersen, G. Kristensson, and A. F. Molisch, "Impact of matching network on bandwidth of compact antenna arrays," *IEEE Transactions on Antennas and Propagation*, vol. 54, pp. 3225 – 3238, Nov. 2006.

[53] S. Blanch, J. Romeu, and I. Corbella, "Exact representation of antenna system diversity performance from input parameter description," *Electronics Letters*, vol. 39, pp. 705 – 707, May 2003.

[54] P. Hallbjörner, "The significance of radiation efficiencies when using s-parameters to calculate the received signal correlation from two antennas," *IEEE Antennas and Wireless Propagation Letters*, vol. 4, pp. 97 – 77, 2005.

[55] S. Dossche, S. Blanch, and J. Romeu, "Optimum antenna matching to minimise signal correlation on a two-port antenna diversity system," *Electronics Letters*, vol. 40, pp. 1164 – 1165, Sep. 2004.

[56] M. Morris and M. Jensen, "Network model for MIMO systems with coupled antennas and noisy amplifiers," *IEEE Transactions on Antennas and Propagation,*, vol. 53, pp. 545 – 552, Jan. 2005.

[57] C. Domizioli, B. Hughes, K. Gard, and G. Lazzi, "Noise correlation in compact diversity receivers," *IEEE Transactions on Communications*, vol. 58, pp. 1426 – 1436, May 2010.

[58] B. Quist and M. Jensen, "Optimal antenna radiation characteristics for diversity and MIMO systems," *IEEE Transactions on Antennas and Propagation,*, vol. 57, pp. 3474 – 3481, Nov. 2009.

[59] V. Plicanic, I. Vasilev, R. Tian, and B. K. Lau, "Capacity maximisation of a handheld MIMO terminal with adaptive matching in an indoor environment," *Electronics Letters*, vol. 47, no. 16, pp. 900–901, 2011.

[60] M. A. Jensen and B. Booth, "Optimal uncoupled impedance matching for coupled MIMO arrays," in *European Conference on Antennas and Propagation (EuCAP)*, Nice, France, Nov. 2006.

[61] R. Tian and B. K. Lau, "Uncoupled antenna matching for performance optimization in compact MIMO systems using unbalanced load impedance," in *IEEE 67th Vehicular Technology Conference (VTC)*, pp. 299 – 303, Singapore, May 2008.

[62] M. Costa, "Writing on dirty paper," *IEEE Transactions on Information Theory*, vol. 29, pp. 439 – 441, May 1983.

[63] J. Zhang, G. Liu, F. Zhang, L. Tian, N. Sheng, and P. Zhang, "Advanced international communications," *IEEE Vehicular Technology Magazine*, vol. 6, pp. 92 – 100, Jun. 2011.

[64] Z. Ni and D. Li, "Effect of fading correlation on capacity of distributed MIMO," in *15th IEEE International Symposium on Personal, Indoor and Mobile Radio Communications (PIMRC)*, vol. 3, pp. 1637 – 1641, Sep. 2004.

[65] M. Alatossava, A. Taparugssanagorn, V.-M. Holappa, and J. Ylitalo, "Measurement based capacity of distributed MIMO antenna system in urban microcellular environment at 5.25 GHz," in *IEEE 67th Vehicular Technology Conference (VTC)*, pp. 430 – 434, Singapore, May 2008.

[66] V. Jungnickel, S. Jaeckel, L. Thiele, L. Jiang, U. Kruger, A. Brylka, and C. von Helmolt, "Capacity measurements in a cooperative MIMO network," *IEEE Transactions on Vehicular Technology*, vol. 58, pp. 2392 – 2405, Jun. 2009.

[67] R. Tian, B. Wu, B. K. Lau, and J. Medbo, "On MIMO performance enhancement with multi-sector cooperation in a measured urban environment," *Electronics Letters*, 2011 (Submitted).

[68] B. Getu and R. Janaswamy, "The effect of mutual coupling on the capacity of the MIMO cube," *IEEE Antennas and Wireless Propagation Letters*, vol. 4, pp. 240 – 244, 2005.

[69] L. J. Chu, "Physical limitations of omni-directional antennas," *Applied Physics*, vol. 19, pp. 1163 – 1175, 1948.

[70] M. Gustafsson, C. Sohl, and G. Kristensson, "Illustrations of new physical bounds on linearly polarized antennas," *IEEE Transactions on Antennas and Propagation*, vol. 57, pp. 1319 – 1327, May 2009.

[71] D. Stancil, A. Berson, J. Van't Hof, R. Negi, S. Sheth, and P. Patel, "Doubling wireless channel capacity using co-polarised, co-located electric and magnetic dipoles," *Electronics Letters*, vol. 38, pp. 746 –747, Jul. 2002.

[72] D. Skaufel, "Dual polarized omnidirectional antenna," Master's thesis, Royal Institute of Technology, KTH, Stockholm, Sweden, 2005.

[73] A. Kandoian, "Three new antenna types and their applications," *Waves and Electrons*, vol. 18, pp. 70W – 74W, Feb. 1946.

[74] A. Alford and A. Kandoian, "Ultra-high frequency loop antennae," *Electrical Communication*, vol. 18, pp. 255 – 265, 1940.

[75] C.-Y. Chiu, J.-B. Yan, and R. Murch, "Compact three-port orthogonally polarized MIMO antennas," *IEEE Antennas and Wireless Propagation Letters*, vol. 6, pp. 619 – 622, Dec. 2007.

[76] G. Gupta, B. Hughes, and G. Lazzi, "On the degrees of freedom in linear array systems with tri-polarized antennas," *IEEE Transactions on Wireless Communications*, vol. 7, pp. 2458 – 2462, Jul. 2008.

[77] A. Konanur, K. Gosalia, S. Krishnamurthy, B. Hughes, and G. Lazzi, "Increasing wireless channel capacity through MIMO systems employing co-located antennas," *IEEE Transactions on Microwave Theory and Techniques*, vol. 53, pp. 1837 – 1844, Jun. 2005.

[78] I. Kovalyov and D. Ponomarev, "Small-size 6-port antenna for three-dimensional multipath wireless channels," *IEEE Transactions on Antennas and Propagation*, vol. 54, pp. 3746 – 3754, Dec. 2006.

[79] L. Lo Monte, B. Elnour, D. Erricolo, and A. Nehorai, "Design and realization of a distributed vector sensor for polarization diversity applications," in *International Waveform Diversity and Design Conference*, pp. 358 – 361, Jun. 2007.

[80] J. Tabrikian, R. Shavit, and D. Rahamim, "An efficient vector sensor configuration for source localization," *IEEE Signal Processing Letters*, vol. 11, pp. 690 – 693, Aug. 2004.

[81] C.-Y. Chiu, J.-B. Yan, R. Murch, J. Yun, and R. Vaughan, "Design and implementation of a compact 6-port antenna," *IEEE Antennas and Wireless Propagation Letters*, vol. 8, pp. 767 – 770, Dec. 2009.

[82] C.-Y. Chiu, J.-B. Yan, and R. Murch, "24-port and 36-port antenna cubes suitable for MIMO wireless communications," *IEEE Transactions on Antennas and Propagation*, vol. 56, pp. 1170 – 1176, Apr. 2008.

[83] R. D. Richtmyer, "Dielectric resonators," *Journal of Applied Physics*, vol. 10, no. 6, pp. 391 – 398, 1939.

[84] J. Van Bladel, "The excitation of dielectric resonators of very high permittivity," *IEEE Transactions on Microwave Theory and Technology*, vol. 23, pp. 208 – 217, Feb. 1975.

[85] J. Van Bladel, "On the resonances of a dielectric resonator of very high permittivity," *IEEE Transactions on Microwave Theory and Technology*, vol. 23, pp. 199 – 208, Feb. 1975.

[86] M. McAllister, S. Long, and G. Conway, "Rectangular dielectric resonator antenna," *Electronics Letters*, vol. 19, pp. 218 – 219, Mar. 1983.

[87] A. Kishk, H. Auda, and B. Ahn, "Accurate prediction of radiation patterns of dielectric resonator antennas," *Electronics Letters*, vol. 23, pp. 1374 – 1375, Dec. 1987.

[88] R. K. Mongia and A. Ittipiboon, "Theoretical and experimental investigations on rectangular dielectric resonator antennas," *IEEE Transactions on Antennas and Propagation*, vol. 45, pp. 1348 – 1356, Sep. 1997.

[89] Z. Ying, "Compact dielectric resonant antenna," *U.S. Patent Application No. 20080122703*, Sep. 22, 2006.

[90] H. Li, Y. Tan, B. K. Lau, Z. Ying, and S. He, "Characteristic mode based tradeoff analysis of antenna-chassis interactions for multiple antenna terminals," *IEEE Transactions on Antennas and Propagation*, 2011 (In press).

[91] K. Karlsson, J. Carlsson, and P.-S. Kildal, "Reverberation chamber for antenna measurements: modeling using method of moments, spectral domain techniques, and asymptote extraction," *IEEE Transactions on Antennas and Propagation*, vol. 54, pp. 3106 – 3113, Nov. 2006.

[92] M. Pelosi, O. Franek, M. Knudsen, G. Pedersen, and J. Andersen, "Antenna proximity effects for talk and data modes in mobile phones," *IEEE Antennas and Propagation Magazine*, vol. 52, pp. 15 – 27, Jun. 2010.

[93] F. Harrysson, J. Medbo, A. Molisch, A. Johansson, and F. Tufvesson, "Efficient experimental evaluation of a MIMO handset with user influence," *IEEE Transactions on Wireless Communications*, vol. 9, pp. 853 – 863, Feb. 2010.

[94] J. Krogerus, P. Suvikunnas, C. Icheln, and P. Vainikainen, "Evaluation of diversity and MIMO performance of antennas from phaseless radiation patterns," in *First European Conference on Antennas and Propagation (EuCAP)*, Nice, France, Nov. 2006.

[95] R. Tian and B. K. Lau, "Simple and improved approach of estimating MIMO capacity from antenna magnitude patterns," in *Third European Conference on Antennas and Propagation (EuCAP)*, Berlin, Germany, Mar. 2009.

[96] R. Tian, B. K. Lau, and Z. Ying, "Multiplexing efficiency of MIMO antennas," *IEEE Antennas and Wireless Propagation Letters*, vol. 10, pp. 183 – 186, 2011.